Laboratory and Field Studies in Sports-Related Brain Injury

Bryan R. Cobb

Dissertation submitted to the faculty of the Virginia Polytechnic Institute and State University in partial fulfillment of the requirements for the degree of

Doctor of Philosophy
In
Biomedical Engineering

Steven Rowson, Chair
Stefan M. Duma, Co-Chair
P. Gunnar Brolinson
F. Scott Gayzik
Joel D. Stitzel

March 25, 2015
Blacksburg, VA

Keywords: Biomechanics, Concussion, Football, Helmet testing, and Head acceleration

Laboratory and Field Studies in Sports-Related Brain Injury

Bryan R. Cobb

ABSTRACT

The studies presented in this dissertation investigated biomechanical factors associated with sports-related brain injuries on the field and in the laboratory. In the first study, head impact exposure in youth football was observed using a helmet mounted accelerometer system to measure head kinematics. The results suggest that restriction on contact in practice at the youth level can translate into reduced head impact exposure over the course of a season. A second study investigated the effect of measurement error in the head impact kinematic data collected by the helmet mounted system have on subsequent analyses. The objective of this study was to characterize the propagation of random measurement error through data analyses by quantifying descriptive statistic uncertainties and biases for biomechanical datasets with random measurement error. For distribution analyses, uncertainties tend to decrease as sample sizes grow such that for a typical player, the uncertainties would be around 5% for peak linear acceleration and 10% for peak angular (rotational) acceleration. The third and fourth studies looked at comparisons between two headforms commonly used in athletic helmet testing, the Hybrid III and NOCSAE headforms. One study compared the headform shape, particularly looking at regions that are likely to affect helmet fit. Major differences were found at the nape of the neck and in the check/jaw regions that may contribute to difficulty with fitting a helmet to the Hybrid III headform. For the final study, the impact responses of the two headforms were compared. Both headforms were mounted on a Hybrid III neck and impacted at various magnitudes and locations that are representative of impacts observed on the football field. Some condition-specific differences in kinematic parameters were found between the two headforms though they tended to be small. Both headforms showed reasonable repeatability.

Table of Contents

List of Figures

List of Tables

Attributions

Several co-investigators made significant contributions to the manuscripts included in this dissertation. Their names and affiliations are listed below by chapter.

Chapter 2: Jillian E. Urban[1,2], Elizabeth M. Davenport[1,2], Steven Rowson[1,3], Stefan M. Duma[1,3], Joseph A. Maldjian[1,4], Christopher T. Whitlow[4,5], Alexander K. Powers[6,7], and Joel D. Stitzel[1,2]

Chapter 3: Steven Rowson[1,3]

Chapter 4: Anna MacAlister[1,3], Tyler J. Young[1,3], Andrew R. Kemper[1,3], Steven Rowson[1,3], Stefan M. Duma[1,3]

Chapter 5: Abigail M. Zadnik[1,3], Steven Rowson[1,3]

Author affiliations: [1]School of Biomedical Engineering and Sciences, Virginia Tech-Wake Forest University; [2]Wake Forest School of Medicine; [3]Department of Biomedical Engineering and Mechanics, Virginia Tech; [4]Department of Radiology (Neuroradiology), [5]Wake Forest School of Medicine; [6]Translational Science Institute, Wake Forest School of Medicine; [7]Department of Neurosurgery, Wake Forest School of Medicine

Chapter 1: Introduction

Sports-related brain injuries have garnered much attention among researchers, medical professionals, and the general public in recent years. As many as 3.8 million sports-related concussions occur each year in the United State, many of which go undiagnosed.[1] Contact and collision sports are responsible for many of these concussions, with football accounting for more than any other organized sport.[2] The long-term consequences of sports-related concussions and even sub-concussive head impacts are not well understood; though, preliminary findings indicate links may exist between repeated head impacts in sports and brain disorders such as depression and chronic traumatic encephalopathy.[3, 4]

Concussion is a mild form of traumatic brain injury (TBI) associated with short-term neurological impairment that is widely believed to be the result of abnormal pressures and strains in the brain caused by forces applied to the head.[5, 6] Numerous biomechanical parameters are associated with abnormal pressures and strains in the brain: acceleration, change in velocity, and impact duration, direction, location, and frequency, among others.[7] As such, these parameters have been employed to characterize concussion biomechanics and assess risk.[8-16] Interventions have been proposed to mitigate the biomechanical parameters associated with concussions in order to reduce injury risk and concussion incidence in sports.[10, 17-19]

Strategies to minimize concussion risk and incidence in sports can be classified into three general categories: rule changes, proper technique, and better equipment.[5, 20] By implementing rules and improving player technique, head impact frequency may be reduced, thereby limiting player exposure to conditions that have potential to cause injury. Some head impacts in sports cannot be avoided all together however, so better equipment is also needed to reduce the severity of impacts that do occur, in order to lower injury risk. Combined, these three strategies can minimize injury risk and lead to fewer sports-related concussions.

Objective Statement

The studies included in this dissertation aim to improve understanding of the biomechanics of head impact exposure in the field and advance laboratory methods for assessing athletic helmets: with the goal of reducing the prevalence of concussions in sports.

Chapter Summaries

Chapter 2: In the first study, 9 to 12 year old youth football players on three teams were instrumented with accelerometer arrays to measure head impact exposure in practices and games. The study presented the first head impact exposure data for football players in this age range and highlighted potential effects of differences in practice structure. Two of the instrumented teams had no restrictions on contact in practices while the third team had restrictions intended to reduce the amount of head impact exposure in practices.

Chapter 3: The next study investigated the affect measurement errors from the head instrumentation employed in the first study have on descriptive statistics used to analyze head impact exposure data. Numerical analyses were conducted using Monte Carlo simulations and subsampling to characterize uncertainties and biases in descriptive statistics of distributions for full datasets, individual players, and teams.

Chapter 4: Moving to laboratory methods, the next study compared the shapes of two common headforms used for helmet testing. Headform shape affects helmet fit in laboratory testing which may affect the impact response and repeatability measures in impact tests. The study highlighted differences between the two headforms in regions that are most likely to affect helmet fit in order to guide researchers in optimal headform selection for future research and evaluation standards related to athletic helmets.

Chapter 5: Headform impact response is also an important consideration for research and evaluation standards related to athletic helmets. In this study, matched impact tests were performed on the same headforms compared in Chapter 4, the Hybrid III and NOCSAE headforms. The headforms were fitted with a football helmet and impacted at various magnitudes and locations using a pendulum impactor to compare the responses for impacts that are representative of those observed in the field. This data will help to guide researchers in the selection of appropriate headforms for future helmet research and evaluation.

Chapter 2: Head Impact Exposure in Youth Football: Elementary School Ages 9 to 12 Years and the Effect of Practice Structure

Abstract

Head impact exposure in youth football has not been well-documented, despite children under the age of 14 accounting for 70% of all football players in the United States. The objective of this study was to quantify the head impact exposure of youth football players, age 9 to 12, for all practices and games over the course of single season. A total of 50 players (age = 11.0 ± 1.1 years) on three teams were equipped with helmet mounted accelerometer arrays, which monitored each impact players sustained during practices and games. During the season, 11,978 impacts were recorded for this age group. Players averaged 240 ± 147 impacts for the season with linear and rotational 95th percentile magnitudes of 43 ± 7 g and 2034 ± 361 rad/s^2. Overall, practice and game sessions involved similar impact frequencies and magnitudes. One of the three teams however, had substantially fewer impacts per practice and lower 95th percentile magnitudes in practices due to a concerted effort to limit contact in practices. The same team also participated in fewer practices, further reducing the number of impacts each player experienced in practice. Head impact exposures in games showed no statistical difference. While the acceleration magnitudes among 9 to 12 year old players tended to be lower than those reported for older players, some recorded high magnitude impacts were similar to those seen at the high school and college level. Head impact exposure in youth football may be appreciably reduced by limiting contact in practices. Further research is required to assess whether such a reduction in head impact exposure will result in a reduction in concussion risk.

Introduction

In recent years, football has come under increased scrutiny because of the concern for player safety and the risk of injury, especially related to concussion. Researchers estimate that between 1.6 and 3.8 million cases of sports related concussion occur each year in the United States, with football having the highest rate of injury among team sports.[1, 2] While the long term effects of sports concussions are still under investigation, links may exist between the accumulation of head impacts over a playing career and increased risk of neurodegenerative diseases later in life, among other health concerns.[3] The majority of the biomechanics research investigating concussions in football has been focused on high school, college, and professional players, despite that more than two-thirds of football players are under the age of 14.[21]

In order to understand the biomechanics associated with concussion, numerous studies have been conducted over the last decade to investigate player exposure and tolerance to head impacts in football.[10-14, 16, 22-32] Many of these studies have utilized commercially available helmet-mounted accelerometer arrays (Head Impact Telemetry (HIT) System, Simbex, Lebanon, NH) to measure head kinematics resulting from head impact in real-time during live play. The accelerometer arrays collect data from each head impact a player experiences while instrumented, allowing researchers to get a more complete view of the biomechanical response of a player's head to impacts across a wide range of magnitudes. Since 2003, more than 1.5 million impacts have been recorded using the HIT System, primarily at the high school and college level.[16, 17, 23, 24, 33] From these data, strategies to reduce head impact exposure through rule changes and methods to evaluate protective equipment have been developed.[10, 16, 17, 24] Unfortunately, little research has focused on youth football, where the head impact exposure is still not well understood.[21] A single study has

investigated head impact exposure at the youth level. That study found that 7 and 8 year old players sustained an average of 107 impacts over the course of a season, with the majority of high magnitude impacts occurring in practice.[21] In response to this research, youth football organizations have made educated recommendations and mandates regarding contact in practice.[18]

An estimated 5 million athletes participate in organized football in the United States annually. Children, age 6 to 13 years, account for around 3.5 million of these participants, compared to just 2000 in the National Football League (NFL), 100,000 in college, and 1.3 million in high school.[21, 34, 35] Despite making up 70% of the football playing population, just one study has investigated head impact exposure experienced by youth football players under 14 years old. The objective of this study was to quantify the head impact exposure of youth football players, aged 9 to 12 years, for all practices and games over the course of single season. These data, along with future research, may be used to develop scientifically based strategies for head injury mitigation.

Materials & Methods

On-field head impact data were collected from 50 players, age 9 to 12 years, on three youth tackle football teams instrumented with the HIT System (Figure 2.1) for a single fall football season. The three teams consisted of a juniors team (team A, 9 to 11 years old), a pee wee team (team B, 10 to 12 years old), and a junior pee wee team (team C, 9 to 11 years old). Further description of the three teams is provided in Table 2.1. Players were monitored during each of the teams' games and contact practices. Approval for this study was given by the Virginia Tech and Wake Forest University Institutional Review Boards (IRBs). Each player provided assent and their parent/guardian gave written consent for participation in the study.

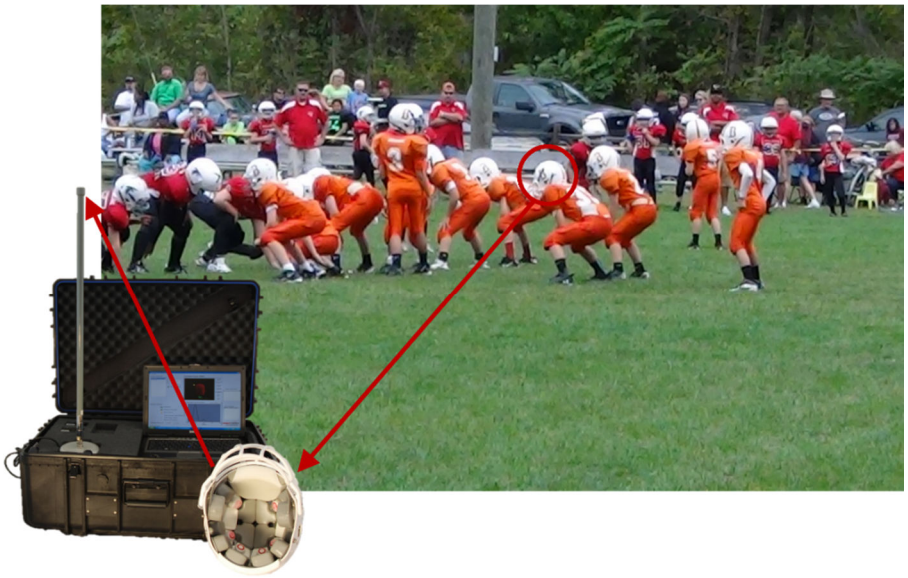

Figure 2.1: HIT System including helmet-mounted accelerometer array (inside helmet) and sideline computer system used for collecting acceleration data during play.

Table 2.1: Description of subject groups investigated in this study.

Team	Player mass (kg)	Player age (years)	Number of players	Number of impacts
A	37.6 ± 5.7	9.8 ± 0.8	14	2206
B	50.1 ± 3.9	12.2 ± 0.5	17	5005
C	43.9 ± 5.9	10.9 ± 0.6	19	4767
Combined	44.2 ± 7.2	11.0 ± 1.1	50	11978

The HIT System consists of an array of 6 non-orthogonally mounted single-axis accelerometers oriented normal to the surface of the head. The arrays, designed to fit in medium or large Riddell Revolution helmets, were installed between the existing padding inside the helmets. Each accelerometer is mounted on an elastic base so that they remain in contact with the head throughout the duration of head impact, allowing for the measurement of head acceleration rather than that of the helmet.[36] Any time an instrumented player experienced a head impact that resulted in a single accelerometer measuring 14.4 g during games and practices, data acquisition was triggered to record 40 ms of data at 1000 Hz, including 8 ms of pre-trigger data. Data from the helmet-mounted

accelerometers were then transmitted wirelessly to a computer on the sideline, where the data were stored and processed to compute resultant linear head acceleration and peak rotational head acceleration using previously described methods.[12, 37] In addition, impact location was generalized into 1 of 4 impact locations (front, side, top, or back) based on the acceleration vectors from the linear accelerometers.[15] Impacts were verified using video from practice and game sessions to ensure they occurred while players were wearing the helmets. The HIT system has previously been found to reliably determine linear acceleration and peak rotational acceleration.[38]

Empirical cumulative distribution functions (CDF) for both linear and rotational head acceleration were determined. Head impact exposure was quantified in terms of impact frequency and 50th and 95th percentile head accelerations. Acceleration duration was measured from the local minimum before peak linear acceleration and the local minimum after the peak, while time to peak linear acceleration was measured from the local minimum before peak linear acceleration to the peak. The data were sorted by generalized impact location and session type (practice or game). A Kruskal-Wallis one-way analysis of variance was conducted to evaluate for between-group differences in head impact exposure associated with the three teams and two session types. A threshold of $p < 0.05$ was used to determine statistical significance. In the event more than two groups were compared, p values were calculated for all pairs and the most conservative p value was reported. All data analysis was conducted on an individual player basis and then averaged to represent the exposure level of a typical 9 to 12 year old football player. Head impact exposure levels were then compared with those of other levels of play that have been previously described in the literature.

Results

A total of 11,978 impacts were measured, ranging from linear accelerations of 10 g to 126 g and rotational accelerations of 4 rad/s^2 to 5838 rad/s^2. The distribution of linear acceleration had a median value of 19 g and a 95th percentile value of 46 g. The distribution of rotational acceleration had a median value of 890 rad/s^2 and a 95th percentile value of 2081 rad/s^2. Cumulative distribution functions of linear and rotational acceleration magnitudes for the season were determined (Figure 2.2). The acceleration distributions are right-skewed and heavily weighted toward lower magnitude impacts. The impact durations measured were 8.82 ± 2.97 ms (average ± standard deviation) with a time to peak linear acceleration of 4.67 ± 1.73 ms. Resultant linear acceleration is plotted vs. time for several impacts recorded in this study as, examples of a typical acceleration pulse (Figure 2.3).

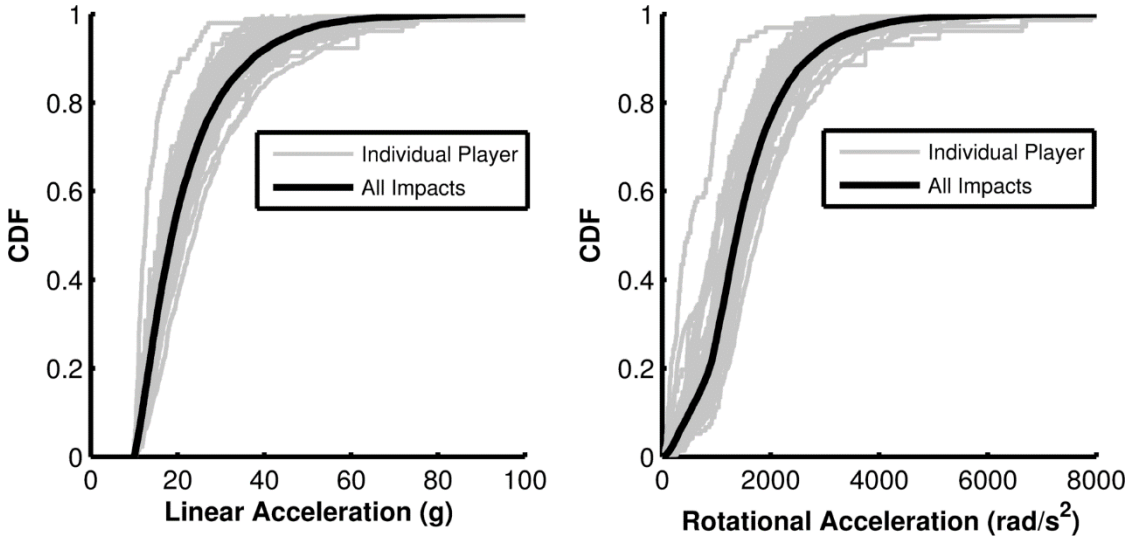

Figure 2.2: Cumulative distribution plots of linear acceleration (left) and rotational acceleration (right) magnitudes for impacts collected during the season.

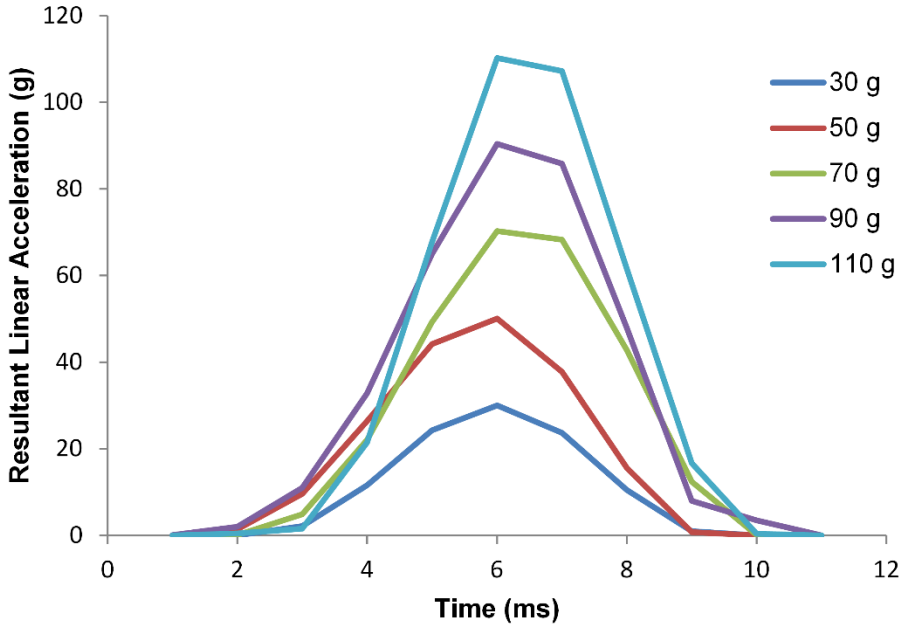

Figure 2.3: Resultant linear acceleration vs. time for several impacts of various magnitudes recorded among 9 to 12 year old football players.

On average, instrumented players sustained 240 ± 147 impacts during the season, with values ranging from 26 to 585 impacts. The average instrumented player sustained 10.6 ± 5.2 impacts per session while participating in 21.8 ± 5.7 sessions. The median impact sustained by instrumented players resulted in accelerations of 18 ± 2 g and 856 ± 135 rad/s^2. The 95th percentile impact sustained by instrumented players resulted in accelerations of 43 ± 7 g and 2034 ± 361 rad/s^2. Head impact exposure was quantified on an individual player basis by session type (Table 2.2). A total of 961 impacts (8.0%) greater than 40 g, 160 impacts (1.3%) greater than 60 g, and 36 impacts (0.3%) greater than 80 g were recorded throughout the season. The average player sustained 19.2 ± 20.1 impacts greater than 40 g, 3.2 ± 4.4 impacts greater than 60 g, and 0.7 ± 1.2 impacts greater than 80 g.

In games, the average player had a median linear acceleration value of 19 ± 2 g and a 95th percentile value of 43 ± 8 g. The average player had a median linear acceleration value of 18 ± 2 g and 95th

percentile value of 40 ± 7 g in practices. Both the difference in median ($p = 0.0289$) and 95th percentile ($p = 0.0463$) linear acceleration magnitudes between games and practices were significant. For rotational acceleration, the average player had a median value of 867 ± 149 rad/s^2 and a 95th percentile value of 2117 ± 436 rad/s^2 for games. In practices, the average player had a median rotational acceleration value of 829 ± 152 rad/s^2 and a 95th percentile value of 1884 ± 385 rad/s^2. As with linear acceleration, the difference between game and practice 95th percentile rotational acceleration ($p = 0.0099$) was significant. The average player sustained 154 ± 113 impacts in 14.4 ± 5.2 contact practices and 85 ± 68 impacts in 7.4 ± 1.2 games. On a per session basis, players experienced 9.7 ± 4.9 impacts per practice and 11.3 ± 8.7 impacts per game. While players experienced significantly more impacts in practices than games ($p = 0.0011$) throughout the season, the difference in the number of impacts per session for practices and games ($p = 0.9423$) was not significant.

Substantial differences existed among the three teams in this study for both impact frequency and acceleration magnitude (Table 2.3). Players on team A accumulated fewer impacts in practices during the season ($p < 0.0001$) than those on teams B and C, as well as fewer impacts on a per practice basis ($p < 0.0097$). Furthermore, team A players sustained appreciably lower magnitude accelerations than their team B and C counterparts (Figure 2.4). For linear acceleration magnitude, the 95th ($p < 0.0001$) percentile differences between team A and the other two was significant for practices. Difference in rotational acceleration magnitudes between team A and teams B and C was significant for the median ($p < 0.0001$) and 95th percentile ($p < 0.002$) values for practices. In games, impact frequency and acceleration magnitudes were not significantly different among the teams. Team A players sustained significantly fewer impacts throughout the season compared to

Table 2.2: Expanded head impact exposure data for each player, split up by session type for each team: (a) team A, (B) team B, and (c) team C.

(a)

	Practice							Games							Season						
		Number of Impacts		Linear Acceleration (g)		Rotational Acceleration (rad/s^2)			Number of Impacts		Linear Acceleration (g)		Rotational Acceleration (rad/s^2)			Number of Impacts		Linear Acceleration (g)		Rotational Acceleration (rad/s^2)	
Player ID	Sessions	Total	Per Session	50%	95%	50%	95%	Sessions	Total	Per Session	50%	95%	50%	95%	Sessions	Total	Per Session	50%	95%	50%	95%
A1	8	53	6.6	14	26	319	982	6	46	7.7	11	17	269	1004	14	99	7.1	13	25	305	1051
A2	3	19	6.3	15	34	667	1247	7	73	10.4	20	53	973	2401	10	92	9.2	17	54	890	2348
A3	8	52	6.5	21	41	996	2019	8	176	22.0	20	42	940	2139	16	228	14.3	20	42	943	2130
A4	10	87	8.7	16	42	448	1915	7	286	40.9	19	46	702	2186	17	373	21.9	18	45	633	2156
A5	9	36	4.0	16	33	647	1321	6	25	4.2	15	44	603	2650	15	61	4.1	16	35	637	1826
A6	10	53	5.3	19	30	770	1530	8	54	6.8	18	33	903	1826	18	107	5.9	19	33	854	1570
A7	8	44	5.5	16	27	642	1489	7	45	6.4	18	35	838	1474	15	89	5.9	17	30	785	1494
A8	9	39	4.3	17	38	698	1891	7	109	15.6	18	45	791	1883	16	148	9.3	18	44	777	1892
A9	7	16	2.3	16	29	669	1392	8	56	7.0	21	58	1114	3310	15	72	4.8	20	53	1002	3115
A10	7	78	11.1	19	32	669	1509	7	160	22.9	17	32	633	1778	14	238	17.0	17	32	664	1738
A11	9	80	8.9	16	30	714	1227	6	160	26.7	16	43	811	2252	15	240	16.0	16	36	780	1796
A12	9	56	6.2	17	36	752	1461	8	96	12.0	19	39	813	2068	17	152	8.9	18	38	774	1953
A13	5	26	5.2	16	33	670	1541	8	61	7.6	18	48	576	2151	13	87	6.7	17	47	613	1724
A14	6	35	5.8	17	32	728	1455	8	185	23.1	18	36	808	1696	14	220	15.7	18	35	788	1696
Ave.	7.7	48	6.2	17	33	671	1499	7.2	109	15.2	18	41	770	2059	14.9	158	10.5	17	39	746	1892
SD	1.9	21	2.1	2	5	147	274	0.8	71	10.1	2	10	199	524	1.9	87	5.3	2	8	166	456

(b)

	Practice							Games							Season						
		Number of Impacts		Linear Acceleration (g)		Rotational Acceleration (rad/s^2)			Number of Impacts		Linear Acceleration (g)		Rotational Acceleration (rad/s^2)			Number of Impacts		Linear Acceleration (g)		rotational Acceleration (rad/s^2)	
Player ID	Sessions	Total	Per Session	50%	95%	50%	95%	Sessions	Total	Per Session	50%	95%	50%	95%	Sessions	Total	Per Session	50%	95%	50%	95%
B1	18	104	5.8	19	34	913	1944	6	9	1.5	23	46	983	2183	24	113	4.7	19	39	920	2077
B2	15	129	8.6	17	48	866	1769	7	21	3.0	22	35	879	1929	22	150	6.8	18	47	874	1796
B3	15	114	7.6	20	41	1018	2020	7	21	3.0	17	36	865	2169	22	135	6.1	19	41	1011	2072
B4	21	338	16.1	21	58	1004	2732	9	199	22.1	25	64	1121	2907	30	537	17.9	22	59	1061	2801
B5	13	146	11.2	21	42	1045	2164	5	25	5.0	18	41	705	1627	18	171	9.5	19	42	994	2083
B6	17	248	14.6	18	45	980	2152	7	74	10.6	21	44	1051	2097	24	322	13.4	19	46	988	2154
B7	8	107	13.4	19	42	864	1660	5	45	9.0	21	48	923	2342	13	152	11.7	19	48	895	1974
B8	18	314	17.4	22	44	974	2159	9	84	9.3	20	45	856	2235	27	398	14.7	21	44	956	2177
B9	15	87	5.8	16	32	788	1606	9	50	5.6	18	36	938	1675	24	137	5.7	17	33	835	1629
B10	15	197	13.1	19	45	861	2059	8	218	27.3	21	50	977	2605	23	415	18.0	19	48	924	2437
B11	14	128	9.1	19	37	969	1693	8	37	4.6	18	35	917	1795	22	165	7.5	18	37	964	1718
B12	18	423	23.5	21	49	900	2001	8	87	10.9	21	48	975	1989	26	510	19.6	21	49	904	2005
B13	21	484	23.0	24	49	1170	2474	8	101	12.6	21	51	1044	2136	29	585	20.2	24	49	1137	2437
B14	18	341	18.9	17	42	734	1901	8	98	12.3	17	48	753	2113	26	439	16.9	17	42	743	1918
B15	16	116	7.3	18	38	859	2151	7	27	3.9	18	36	888	1958	23	143	6.2	18	38	881	2128
B16	18	192	10.7	16	35	834	1808	7	40	5.7	18	46	923	2411	25	232	9.3	16	37	837	1881
B17	19	246	12.9	19	48	904	2177	7	155	22.1	20	52	935	2459	26	401	15.4	19	50	915	2379
Ave.	16.4	218	12.9	19	43	923	2028	7.4	76	9.9	20	45	925	2155	23.8	294	12.0	19	44	932	2098
SD	3.0	119	5.4	2	6	102	282	1.2	61	7.3	2	7	99	319	3.9	159	5.2	2	6	90	284

(c)

	Practice							Games							Season						
		Number of Impacts		Linear Acceleration (g)		Rotational Acceleration (rad/s^2)			Number of Impacts		Linear Acceleration (g)		Rotational Acceleration (rad/s^2)			Number of Impacts		Linear Acceleration (g)		Rotational Acceleration (rad/s^2)	
Player ID	Sessions	Total	Per Session	50%	95%	50%	95%	Sessions	Total	Per Session	50%	95%	50%	95%	Sessions	Total	Per Session	50%	95%	50%	95%
C1	18	258	14.3	19	43	931	1873	6	67	11.2	20	45	989	1954	24	325	13.5	19	44	940	1951
C2	22	377	17.1	20	47	1012	2511	8	191	23.9	23	49	1152	2411	30	568	18.9	21	47	1050	2463
C3	18	152	8.4	16	37	825	1766	9	36	4.0	16	37	837	1537	27	188	7.0	16	37	835	1690
C4	17	125	7.4	18	41	858	1866	7	85	12.1	18	44	821	2449	24	210	8.8	18	43	850	2179
C5	18	143	7.9	17	38	842	2137	8	56	7.0	16	31	748	1687	26	199	7.7	16	36	818	1911
C6	21	286	13.6	17	46	852	2164	9	244	27.1	20	47	945	2128	30	530	17.7	19	47	898	2153
C7	17	154	9.1	18	39	874	1765	7	30	4.3	19	32	852	1444	24	184	7.7	18	38	874	1745
C8	18	125	6.9	16	37	757	1519	5	19	3.8	17	50	731	2654	23	144	6.3	16	38	755	1844
C9	18	171	9.5	18	47	925	2321	8	33	4.1	17	27	882	1624	26	204	7.8	18	46	921	2276
C10	21	283	13.5	17	40	801	1587	8	114	14.3	19	40	851	1895	29	397	13.7	18	40	821	1652
C11	17	187	11.0	17	37	823	1778	8	122	15.3	19	34	888	1772	25	309	12.4	18	36	845	1783
C12	20	148	7.4	17	51	745	2196	9	55	6.1	17	43	783	2224	29	203	7.0	17	49	759	2206
C13	16	155	9.7	18	47	876	2190	7	84	12.0	19	51	1001	1926	23	239	10.4	19	48	957	2073
C14	19	210	11.1	18	40	894	2190	8	30	3.8	18	47	976	2662	27	240	8.9	18	40	899	2254
C15	21	122	5.8	19	54	929	2705	9	26	2.9	18	50	824	2387	30	148	4.9	19	54	885	2715
C16	18	268	14.9	20	42	985	2100	9	177	19.7	19	47	921	2307	27	445	16.5	20	44	946	2140
C17	15	66	4.4	21	48	1013	2180	8	46	5.8	20	51	913	2344	23	112	4.9	21	50	963	2367
C18	13	81	6.2	16	36	765	1464	5	15	3.0	20	37	967	1724	18	96	5.3	17	37	780	1601
C19	7	17	2.4	15	47	681	2456	5	9	1.8	15	57	777	3259	12	26	2.2	16	56	742	2565
Ave.	17.6	175	9.5	18	43	863	2040	7.5	76	9.6	18	43	887	2126	25.1	251	9.5	18	44	870	2083
SD	3.3	85	3.8	2	5	89	334	1.4	64	7.3	2	8	101	451	4.3	141	4.6	1	6	80	311

Table 2.3: Summary comparison of three teams of 9 to 12 year old players.

	Practices						Games						Season					
	Impacts		Linear acceleration (g)		Rotational acceleration (rad/s^2)		Impacts		Linear acceleration (g)		Rotational acceleration (rad/s^2)		Impacts		Linear acceleration (g)		Rotational acceleration (rad/s^2)	
Team	Total	Per session	Median (50%)	95%	Median (50%)	95%	Total	Per session	Median (50%)	95%	Median (50%)	95%	Total	Per session	Median (50%)	95%	Median (50%)	95%
A	48	6.2	17	33	671	1499	109	15.2	18	41	770	2059	158	10.5	17	39	746	1892
B	218	12.9	19	43	923	2028	76	9.9	20	45	925	2155	294	12.0	19	44	932	2098
C	175	9.5	18	43	863	2040	76	9.6	18	43	887	2126	251	9.5	18	44	870	2083

team B players (p = 0.0045) due to practice differences. The difference in head impacts for the season between team A and team C players was not significant (p = 0.0742).

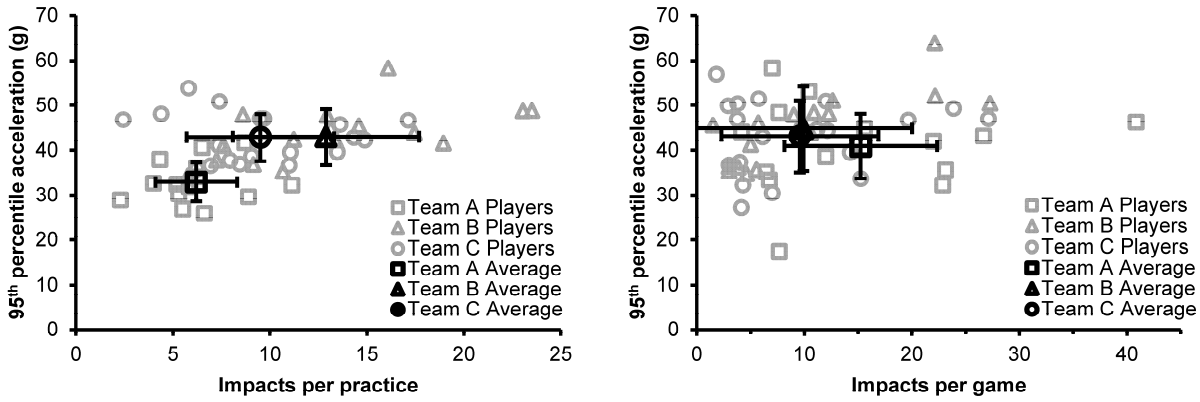

Figure 2.4: Player 95th percentile acceleration magnitude vs. number of impacts per session for practices (left) and games (right). Individual players are shown in gray while team averages are displayed in black with error bars showing standard deviation.

Impacts to the front of the helmet were the most common, representing 41% of all impacts, followed by those to the back at 25% and side at 23% (Table 2.4). The least frequently impacted location was the top of the helmet, representing 11% of all impacts. Impacts to the top of the helmet resulted in the highest magnitude linear accelerations with a median value of 21 g and a 95th percentile value of 46 g. For rotational acceleration, impacts to the front had the highest values while those to the top had the lowest.

Among the three teams participating in this study, four instrumented players sustained concussions diagnosed by physicians: two on the pee wee team (B4 and B6) and one on each of the other two teams (A8 and C18). The impact associated with player A8's concussion was to the front of the helmet and had a linear acceleration of 58 ± 9 g and rotational acceleration of 4548 ± 1400 rad/s^2.

For player B4, the concussion was associated with an impact to the back of the helmet with linear and rotational acceleration magnitudes of 64 ± 10 g and 2830 ± 900 rad/s^2. No impacts were recorded for B6 on the day of his concussion due to a battery failure in the sensor array. Player C18's concussion was linked to an impact to the side of the helmet with linear and rotational acceleration magnitudes of 26 ± 4 g and 1552 ± 500 rad/s^2.

Table 2.4: Head impact frequency and magnitude by location for 9 to 12 year old players.

	Percentage of impacts	Linear acceleration (g)		Rotational acceleration (rad/s^2)	
Location	(%)	50th	95th	50th	95th
Front	52	19	41	951	2049
Side	19	16	34	810	1715
Rear	18	18	41	790	2030
Top	10	21	46	388	1040

Discussion

Previous studies have investigated the frequency and magnitude of head impacts in other tackle football populations, including youth (7 to 8 years), high school (14 to 18 years), and college (18 to 23 years) in the last decade (Table 2.5).[11, 12, 15, 21] Data from these studies show a trend of increasing acceleration magnitude and impact frequency with increasing level of play. Not surprisingly, the 9 to 12 year old players in this study were found to experience linear acceleration magnitudes between those found in 7 to 8 year old players and high school players. For rotational acceleration, the 95th percentile magnitude found in this study was less than that found previously in younger players.[21] Rotational acceleration tends to correlate well with linear acceleration, though impact location can heavily influence the relationship.[12] Players in this study experienced more impacts to the front of their helmets and fewer to the side than the 7 to 8 year old players studied by Daniel et al.[21] In that study, impacts to the front of player's helmets were associated

with lower rotational acceleration magnitudes, while those to the side were associated with higher magnitudes.

As with magnitude, the impact frequency reported in this study fell between those of 7 to 8 year old and high school athletes. In this study, the average player experienced 240 impacts throughout the season compared to 107 impacts per season for 7 to 8 year old players and 565 for high school players.[14, 15, 21] This trend can be partially attributed to the number of sessions (practices and games) increasing as the level of play increases. The 7 to 8 year old team studied by Daniel et al.[21] experienced impacts in 9.4 practices and 4.7 games for a total of 14.1 sessions. Players in this study participated in an average of 14.4 contact practices and 7.4 games, for a total of 21.8 sessions. Compared to the high school team studied by Broglio et al.[14], the teams in this study participated in fewer practices and games in addition to experiencing fewer impacts per session. High school players experienced on average 15.9 impacts per session whereas the 9 to 12 year old players in this study experienced 10.6 impacts per session. The age related differences reported among these three age groups are most likely due to increased size, athleticism, and aggression in older players.

Table 2.5: Comparison of head impact exposure across various levels of play.[11, 12, 14, 15, 21]

		Linear acceleration (g)		Rotational acceleration (rad/s^2)	
Level of play	Number of impacts per season	Median (50%)	95%	Median (50%)	95%
Youth (7-8 years)	107	15	40	672	2347
Youth (9-12 years)	240	18	43	856	2034
High School(14-18 years)	565	21	56	903	2527
College (19-23 years)	1000	18	63	981	2975

Players experienced slightly greater impact frequencies and acceleration magnitudes in games than in practice, similar to findings of high school and college football studies.[16, 22, 23, 39] For example, a group of high school players, experienced a mean linear acceleration magnitude of 23 g in practices and 25 g in games while the players in this study had a mean linear acceleration magnitude of 22 g in practices and 23 g in games.[15] With regard to impact frequency, players in this study experienced a similar number of impacts per practice as per game. The rate of impact in practice was similar to the 9.2 impacts per practice that Broglio et al.[15] reported for high school football players. However, the high school players sustained 24.5 impacts per game. These data suggest that high school players experience fewer impacts in practice than in games, while the 9 to 12 year old players in this study had roughly equal numbers of impacts per session for the two session types.

Substantial differences in impact frequency were observed between team A and the other two teams. For the entire season, players on team A experienced an average of 37-46% fewer impacts than players on teams B and C, though only the difference between teams A and B was statistically significant. This difference is largely due to players on teams B and C participating in 2.1-2.3 times more contact practices than players on team A. The average number of games each player participated in was nearly the same for all three teams, and team A actually had the highest average number of impacts per game at 15.2. Team B and C players averaged 9.9 and 9.6 impacts per game, respectively. Since team A had fewer players than the other two teams, their players may have had more playing time leading to more impacts per game, though other factors such as playing style or skill may have also played a role. For practices, team A players averaged just 6.2 impacts per session compared to 12.9 and 9.5 for teams B and C. Furthermore, players from teams B and

C participated in twice as many practice sessions as those from team A. As a result of the higher rate of impact in practices and greater number of practices, team B and C players experienced 219 and 175 impacts during practices, while team A players averaged 48 impacts.

Several factors may have played a role in reducing the head impact exposure observed in team A players relative to teams B and C in this study. First, Pop Warner mandated two rule changes for the 2012 football season that applied to all of their affiliates: (1) a mandatory minimum play rule, where coaches are required to give each player a certain amount of playing time, and (2) a limit on contact in practice, where no more than one-third of weekly practice time and no more than 40 minutes of a single session can involve contact drills.[18] While no team in this study was affiliated with Pop Warner, the league in which team A competed enforced the same rule changes, whereas teams B and C had no such restrictions. Second, special teams plays, including kickoffs and punts, were live plays for teams B and C, similar to high school, college, and professional football. Alternatively, team A's special teams plays were controlled situations where no contact was allowed. Data from previous studies suggest that players on special teams are more susceptible to large magnitude head accelerations, which may lead to higher incidence of concussion on these plays.[34, 40, 41] Third, all three teams played approximately the same number of games during the season, but Teams B and C played 11 and 12 week seasons while team A had a 9 week season. With more time between games, teams generally practice at a higher frequency and intensity. Fourth, player skill, athleticism, and maturity could have implications on the level of exposure. Even within teams, variability among players is apparent, with some players experiencing substantially more impacts than the team average. No significant differences were found in game acceleration magnitudes or impact frequency, suggesting practice differences were not due to

player differences among teams. Instrumented players ranged from experiencing 72 to 585 head impacts. Fifth, coaching style has major influence on factors such as the types of drills used in practice and the plays called in games. These coaching variations would likely contribute to the differences in the head impact exposure that players experienced.

Two of the impacts (A8 and B4) associated with diagnosed concussions were substantially greater than the player's season 95th percentile linear acceleration magnitude. Furthermore, the acceleration magnitudes were consistent with concussive values reported in previous studies, albeit at the lower end of the range.[11-13] For player A8, the impact was the third highest linear acceleration magnitude he experienced during the season and second highest magnitude resulting from an impact to the front of the helmet. The two highest magnitude impacts that this player experienced were similar in magnitude to the concussive impact. For player B4, the concussive impact was his highest magnitude impact to the back of the helmet for the season. This player also accumulated the third highest number of impacts during the season among all study participants. The third impact associated with a concussion (C18) was in the top 20% of linear acceleration magnitudes for that player throughout the season. Although the acceleration magnitude was relatively low for a concussion, it was the player's second highest magnitude resulting from an impact to the side of the helmet.

The data collected in this study may have applications towards improving the safety of youth football through rule changes, coach training, and equipment design. Prior to the 2012 season, many youth football organizations, including the league in which team A competed, modified rules and provided coaches with practice guidelines to reduce head impacts in practice. The data

collected in this study suggest that head impact exposure over the course of a season can be reduced significantly by limiting contact in practices to levels below those experienced in games. In addition to guiding future rules for youth football, this study can be used to aid designers in developing youth-specific football helmets that may be able to better reduce head accelerations due to head impacts for young football players. Impact location, frequency, and head acceleration magnitudes can be used to optimize helmet padding to maximize protection while keeping factors such as helmet size and mass to age appropriate levels.

A number of limitations should be noted about this study. First, the HIT system used for data collection is associated with some measurement error for linear and rotational acceleration. On average, the HIT system overestimates linear acceleration by 1% and rotational acceleration by 6% when compared to the Hybrid III headform. The correlation between the HIT system and Hybrid III measurements of head acceleration is $R^2 = 0.903$ for linear acceleration and $R^2 = 0.528$ for rotational acceleration.[38] Individual data points have uncertainty values due to random error as well; however, the analysis presented here primarily examined distributions of data sets, rather than individual points. Uncertainty values that account for the random error are included with the three concussive data points presented. Second, this study followed three teams consisting of 9 to 12 year old players with a total of 50 players with large variations in head impact exposure among the different teams and players. Head impact exposure is likely dependent on other factors, in addition to age.

Real-time head impact kinematic data were collected from youth football players, age 9 to 12 years, during practice and game sessions for an entire season. The data show, on average, that

players experienced greater head impact exposure, through more frequent and higher magnitude impacts, than 7 to 8 year old players, but less than that of high school players. Furthermore, players experienced similar levels of head impact exposure in practice and game sessions on a per-session basis. The vast majority of head impacts recorded in both games and practices were below acceleration magnitudes generally associated with concussions; though, some high magnitude impacts, similar to those seen among older players, did occur. The data presented in this study suggest that head impact exposure at the youth level may effectively be reduced by limiting contact in practices. Future studies are required to determine how rule modifications, coaching style, and other factors influence player impact exposure in practice. Furthermore, additional research is required to determine how reducing head impact exposure in practice affects concussion risk in youth football. Researcher should continue to collect head impact kinematic data in youth football across all age groups to establish the level of head impact exposure a typical player experiences, in a season and career, in order to improve player safety in youth football.

Acknowledgements

The authors would like to thank the Childress Institute for Pediatric Trauma at Wake Forest Baptist Medical Center and the National Highway Traffic Safety Administration for providing support for this study as well as Elizabeth Lillie, Matt Bennett, Amanda Dunn, and the South Fork Panthers and Blacksburg youth football programs for their involvement.

Chapter 3: Quantifying the Effects of Random Measurement Error on Descriptive Statistics of Biomechanical Datasets

Abstract

Biomechanical measurements taken in the field can be subject to random measurement error due to the difficulty of instrumenting live human subjects. The objective of this study was to characterize the propagation of random measurement error through data analyses by quantifying descriptive statistic uncertainties and biases for biomechanical datasets with random measurement error. Descriptive statistic uncertainties and biases in peak linear and rotational accelerations were estimated numerically for two biomechanical datasets from the literature using Monte Carlo and resampling techniques. Random measurement error values were based on data from validation studies published in the literature. Uncertainties were found to be a function of sample size, where larger sample sizes corresponded to lower uncertainties. In distribution analyses, random measurement errors of individual data points tend to be counterbalanced by random measurement errors of neighboring data points, with larger sample sizes leading to more complete compensation. While bias was shown to not be affected by sample size, the effects of bias were small and can be accounted for when necessary. Researchers should be mindful of the limitations of biomechanical field data and interpret such data appropriately, as it can be subject to higher random measurement error than data collected in the laboratory.

Introduction

Accurate biomechanical measurements of real-life events can be difficult to obtain due to challenges associated with the instrumentation of human subjects in the field. These challenges may lead to larger random measurement errors (RME) than those typically found in controlled laboratory experiments. Observations from such events, however, can be invaluable in the study of injury biomechanics because they allow researchers the opportunity to observe conditions that cannot be reproduced in the laboratory.

This study focuses on two sets of traumatic brain injury (TBI) data as an illustrative example of datasets containing RME. TBI has garnered much attention in recent years, both in the general populace and among researchers, due in large part to its prevalence in sports, where as many as 3.8 million incidences occur every year.[1, 5, 13, 15, 16, 42] Concussion is the most common form of TBI in sports and is especially prevalent among athletes in collision sports. Concussions are particularly challenging to study because they are a physiological injury that can only be detected in living subjects. Four basic experimental methodologies have been used to study concussions: cadaver, animal, anthropomorphic test device (crash test dummy), and human volunteer models.[6, 8, 28, 43] Each method has advantages and disadvantages; however, only human volunteer studies offer researchers the ability to observe a physiologic injury response in humans. Human volunteers from high-risk populations can be instrumented and observed in the field, allowing researchers to identify biomechanical factors associated with injury. The instrumentation used must be small, light-weight, durable, and untethered so as to minimize interference with normal subject activity while collecting data, all of which add to the challenge of collecting accurate data.

Researchers have instrumented human volunteers in sports associated with elevated concussion risk using accelerometers to characterize head impact kinematics; these sports include football, hockey, boxing, and soccer.[8, 9, 13, 21, 22, 26, 44-51] Helmet-mounted sensor systems have been developed to study brain injury in military service members as well, measuring head acceleration, blast pressures, and other parameters that may be associated with injury risk.[52] Alternative methodologies such as video reconstruction have also been used to characterize head impact biomechanics in sports.[28, 53] While data collected using all of these methodologies have contributed tremendously to the body of knowledge of traumatic brain injury, they often produce data that have relatively high RME compared to controlled laboratory tests, typically greater than 10% for one standard deviation (SD). Field observations capture events that may not be reproducible in the laboratory, such as head accelerations associated with brain injury in humans. The benefits of observing such events in the field may outweigh the drawback of RME.

In this study, the aim was to elucidate how RME propagates through distribution analyses by quantifying descriptive statistic uncertainties and biases for biomechanical datasets with RME. The results will demonstrate how measurement error affects the descriptive statistics commonly used in analyses of biomechanical field data, which will help researchers in future studies manage uncertainties and biases appropriately.

Materials & Methods

Two previously published biomechanical datasets were analyzed to assess descriptive statistic uncertainties and biases using Monte Carlo and resampling techniques: (1) laboratory

reconstructions of concussive National Football League (NFL) head impacts and (2) on-field head impacts in youth football (Figure 3.1).[28, 54, 55] The NFL dataset consisted of normally distributed peak resultant linear and rotational accelerations from 25 concussive impacts reconstructed using helmeted Hybrid III crash test dummies. Measured linear acceleration values ranged from 48 g to 138 g with a median of 101 g. For rotational acceleration, values ranged from 2615 rad/s^2 to 9678 rad/s^2 with a median of 6750 rad/s^2. The on-field dataset consisted of right-skewed distributions of peak resultant linear and rotational accelerations from 4432 head impacts observed using helmet-mounted accelerometer arrays. Head impacts were collected from 25 players during youth football practices and games over the course of one season using the Head Impact Telemetry (HIT) system. Linear acceleration values ranged from 10 g to 116 g with a median of 18 g. Rotational acceleration values ranged from 4 rad/s^2 to 4886 rad/s^2 with a median of 810 rad/s^2.

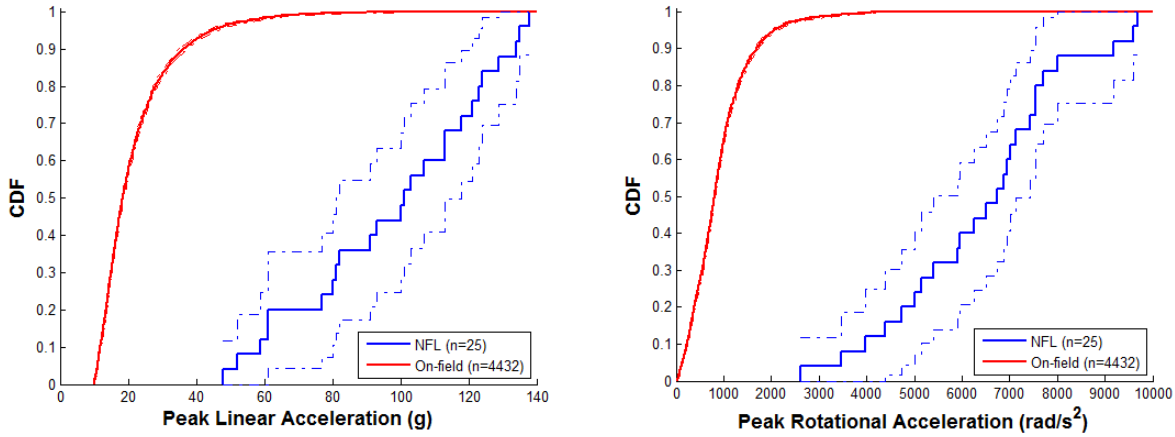

Figure 3.1: Cumulative distribution functions (CDF) of the NFL (blue) and on-field (red) datasets for peak linear acceleration (left) and peak rotational acceleration (right). The confidence intervals of each CDF are shown with dotted lines.

Random measurement error (RME) values were estimated in previous validation studies for the methods employed with the NFL dataset and the HIT System used to collect the on-field data. The validation study for the NFL methods estimated the RME of the peak resultant linear accelerations to be ±11.4% and that of the peak resultant rotational accelerations to be ±17.0%.[56] For the HIT System, the validation study found a RME of ±15.7% for peak resultant linear acceleration measurements and ±31.7% for peak resultant rotational acceleration estimates.[38] Illustrative analyses were also carried out using 50% lower and 50% higher RME in order to evaluate the sensitivity of uncertainty and bias values to changes in RME (Table 3.1).

Table 3.1: Random measurement error (RME) values modeled in this study to evaluate descriptive statistic uncertainties for the NFL and on-field biomechanical datasets.

Dataset	Acceleration	Reduced RME	Published RME	Increased RME
NFL	Linear	5.7%	11.4%	17.1%
	Rotational	8.5%	17.0%	25.5%
On-field	Linear	7.9%	15.7%	23.6%
	Rotational	15.9%	31.7%	47.6%

Descriptive statistics, which are commonly used to characterize distributions of data, were determined for the NFL and on-field datasets in the form of percentiles, ranging from the 5th to the 95th. The 50th percentile is generally used to represent the central tendency of non-normal, unimodal distributions, while the 5th and 95th percentile may be used as measures of dispersion. Each of these statistics has an inherent uncertainty due to measurement error. The effects of RME on descriptive statistic uncertainties and biases were analyzed to answer three questions:

1. What is the uncertainty due to RME associated with impact percentiles in each biomechanical dataset?
2. How does varying sample size affect these uncertainty estimates for impact percentiles in each dataset?
3. How do these errors propagate through aggregate analyses of multiple data distributions?

Uncertainty in Published Datasets

Descriptive statistic uncertainties and biases were estimated for the NFL and on-field datasets for percentiles ranging from the 5th to the 95th, using a Monte Carlo method, as outlined by the following procedure:

1. Acceleration magnitude percentiles ranging from the 5th to 95th were computed in increments of two for both of the published datasets.
2. Monte Carlo simulations were generated by adding RME to each data point in the published datasets. For each data point, RME was modeled with a normal distribution about that point having a standard deviation defined by the published error estimates (Table 3.1). A measurement error value was randomly selected from this normal distribution and assigned the data point. This process was repeated for every point in the datasets to produce each simulation and repeated to generate many simulations.
3. For each simulation, acceleration magnitude percentiles ranging from the 5th to 95th were computed in increments of two.
4. The standard deviation and mean of the simulation descriptive statistics were computed for each percentile. The standard deviation of each percentile was used to estimate uncertainty

due to RME. The difference between the mean of the simulations and published dataset value for each percentile was used to estimate bias due to RME. Enough simulations were generated in Step 2 such that stable solutions for uncertainties and biases were obtained. The process was also repeated for both lower and higher measurement error values (Table 3.1).

Effect of RME as a Function of Sample Size

Subsequent analyses were conducted to assess the effect of sample size on the uncertainties and biases of descriptive statistics due to RME for the NFL and on-field datasets. Uncertainties and biases were quantified for percentiles ranging from the 5th to the 95th for sample sizes from 25 to 2000 data points. This range of sample sizes is representative of the number of head impacts football players from the youth to the college level may experience in a season.[16, 21, 46, 49, 54]

For the on-field data, subsets were generated using uniform random sampling with replacement from the full dataset in order to estimate uncertainties and biases using the following procedure:

1. Datasets consisting of 25, 50, 100, 250, 500, 1000, and 2000 impacts were generated using uniform random sampling with replacement. Enough datasets were generated for each sample size so as to ensure a diverse and representative sample.
2. Acceleration magnitude percentiles ranging from the 5th to 95th were determined in increments of two for each generated dataset.
3. Similar to Step 2 in the previous section, Monte Carlo simulations were generated for each dataset using published error values (Table 3.1).

4. For each simulation, acceleration magnitude percentiles ranging from the 5th to 95th were determined in increments of two.
5. Standard deviations and means of corresponding simulation descriptive statistics were computed by generated dataset. The standard deviation of each percentile was used to estimate uncertainty due to RME for each generated dataset. The difference between the mean of the simulations and published dataset value for each percentile was used to estimate bias due to RME for each generated dataset. Uncertainty values were normalized based on the descriptive statistic values of the generated datasets determined in Step 2.
6. The standard deviations and means were then averaged by sample size to estimated uncertainty and bias for each sample size. In Step 3, enough simulations were generated such that stable uncertainties and biases were obtained.

For the NFL data, a normal distribution was assumed based on the mean and standard deviation of the dataset to compensate for the small sample size of the original dataset. Sample sets of 25, 50, 100, 250, 500, 1000, and 2000 impacts were then generated based on the assumed normal distribution in order to estimate uncertainties and biases using Steps 2-6 of the procedure outlined for the on-field data. The procedure was also repeated for lower and higher measurement error values (Table 3.1).

Analysis of Multiple Distributions

In the final set of analyses, propagation of RME through aggregate analyses of multiple distributions was investigated. Specifically with on-field experiments, data are collected from multiple players, each with their own distribution of head impacts and averaged together to assess

team head impact exposure. Analyses were carried out to investigate the effect of team size on team descriptive statistic uncertainties and biases due to RME. Descriptive statistic uncertainties were estimated for percentiles ranging from the 5th to the 95th for team sizes from 2 to 200 players using the following procedure:

1. A set of players was generated using uniform random sampling with replacement from the on-field dataset. Players were assigned a number of head impacts based on a distribution consistent with field observations. Each player was assigned 178 ± 144 head impacts and players with impact totals outside of one standard deviation were removed from the player set. Enough players were generated to ensure a diverse and representative player set.
2. Acceleration magnitude percentiles ranging from the 5th to 95th were determined in two percentile increments for each generated player.
3. Teams consisting of 2, 5, 10, 25, 50, 100, and 200 players were generated using uniform random sampling of the players generated in the Step 1.
4. Team descriptive statistics were computed by averaging corresponding percentile values determined in Step 2 for the players on each team.
5. Similar to Step 2 in the first analysis procedure, Monte Carlo simulations were generated for each player on each team based on published measurement error values (Table 3.1).
6. Acceleration magnitude percentiles ranging from the 5th to 95th were determined in two percentile increments for each simulation.
7. For each team, descriptive statistics were averaged by corresponding simulation for each percentile (i.e. descriptive values were averaged for the n-simulations of each player on a given team).

8. The standard deviation of the simulation descriptive statistics were computed for each percentile by team to estimate the uncertainty in descriptive statistics for each simulated team. Uncertainty values were normalized based on the descriptive statistic values of the generated teams determined in Step 4.
9. The uncertainty estimates were then averaged among all simulated teams of the same size to represent the average uncertainty due to RME for a team of that size. In steps 2, 3, and 5, enough players, teams, and simulations were generated such that stable uncertainties and obtained. The procedure was also repeated for lower and higher measurement error values (Table 3.1).

Results

Uncertainty in Published Datasets

Descriptive statistic uncertainty and bias estimates of the two datasets were found to be dependent on percentile and random measurement error (RME) value (Figures 3.2 and 3.3). For the NFL dataset, the published RME of 11.7% resulted in maximum uncertainties of 7.5 g for linear acceleration and 800 rad/s^2 for rotational acceleration, with both maximum values associated with the 95th percentiles. The NFL uncertainty and bias curves in Figures 3.2 and 3.3 were smoothed using a five-point moving average to better represent the overall trends as a function of percentile. The maximum uncertainties for the on-field dataset were 0.5 g for linear acceleration and 33 rad/s^2 for rotational acceleration and were also associated with the 95th percentiles. Increased or decreased RME resulted in a corresponding increase or decrease in uncertainties for linear and rotational acceleration values at all percentiles for both datasets. The most apparent differences

were found at the 95th percentiles; for the NFL data, a 50% increase in RME resulted in maximum uncertainties of 10.4 g for linear acceleration and 1070 rad/s^2 for rotational acceleration. The maximum biases estimated using the published RME values were 8.6 g and 536 rad/s^2 for the NFL dataset and 1.6 g and 197 rad/s^2 for the on-field set. All maximum bias values were associated with the 95th percentiles.

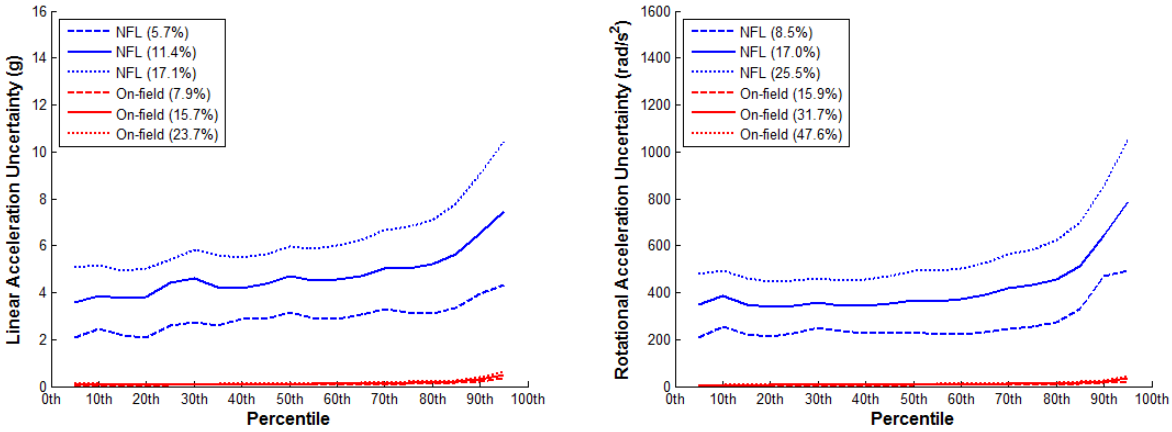

Figure 3.2: Uncertainty due to RME as a function of linear (left) and rotational (right) acceleration percentile for the NFL (blue) and on-field (red) datasets.

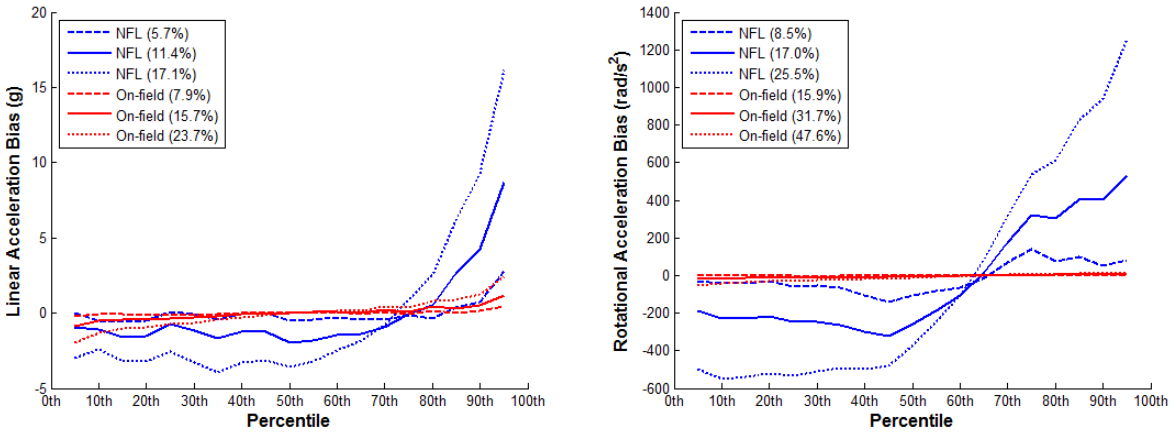

Figure 3.3: Bias due to RME as a function of linear (left) and rotational (right) acceleration percentile for the NFL (blue) and on-field (red) datasets.

Effect of RME as a Function of Sample Size

Descriptive statistic uncertainties varied with sample size (number of impacts in the distribution), with larger sample sizes associated with lower uncertainties (Figure 3.4). The central percentiles tended to have lower normalized uncertainties compared to the low and high percentiles.

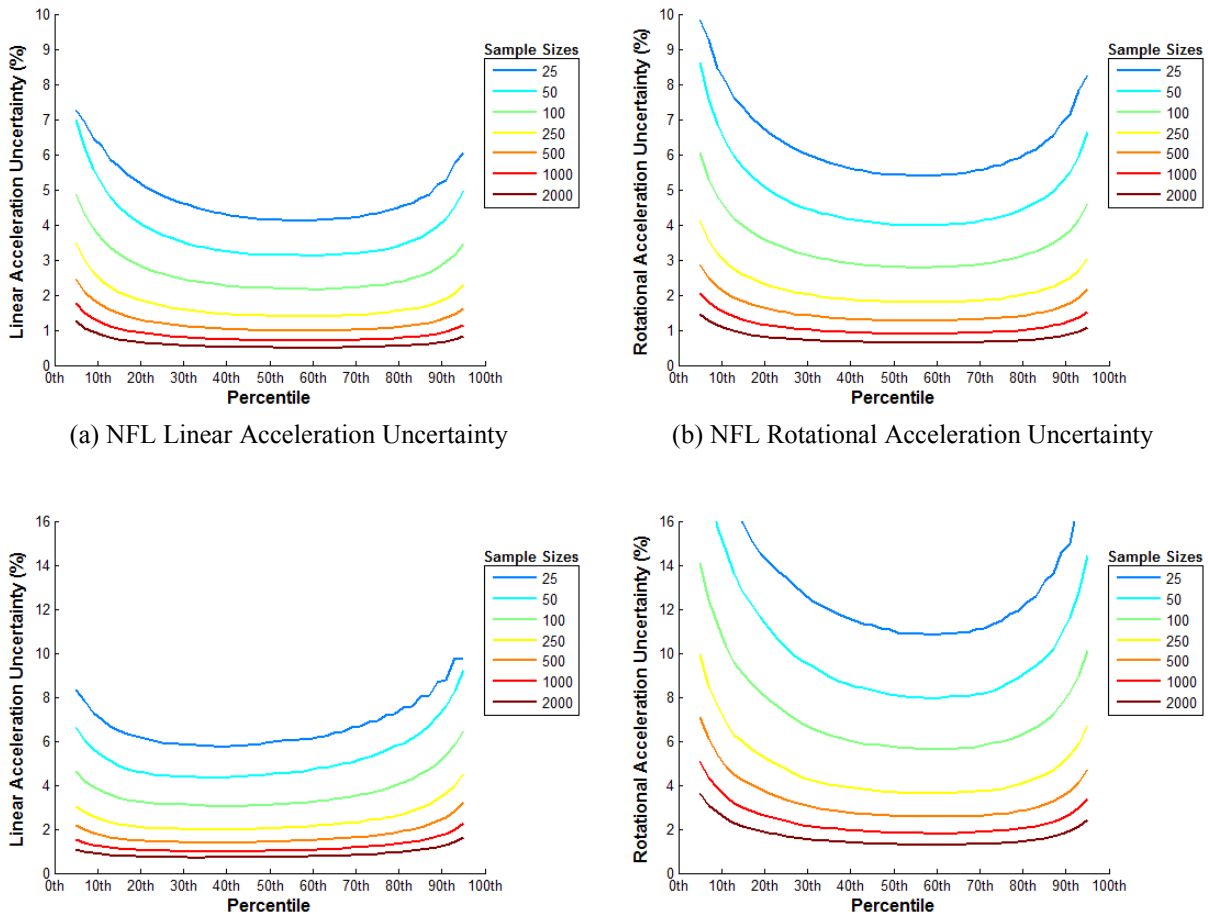

(a) NFL Linear Acceleration Uncertainty

(b) NFL Rotational Acceleration Uncertainty

(c) On-field Linear Acceleration Uncertainty

(d) On-field Rotational Acceleration Uncertainty

Figure 3.4: Uncertainty in linear (left) and rotational (right) acceleration percentiles for the NFL (top) and on-field (bottom) data for sample sizes ranging from 25 to 2000 samples. Larger sample sizes were associated with lower uncertainties.

Using the published RME values, the NFL data 50th percentile uncertainties ranged from 5.8% to 0.5%, while 95th percentile values ranged from 9.1% to 0.8% for sample sizes ranging from 25 to 2000 samples. The on-field data 50th percentile uncertainties ranged from 8.2% to 0.7% and 95th percentile values ranged from 14.0% to 1.6% for the same sample size range. Similar findings were evident with the rotational acceleration uncertainties, though larger uncertainties were associated with corresponding sample sizes. Bias was not substantially affected by sample size (Figure 3.5). For the NFL data, the maximum biases were approximately 6 g and 800 rad/s^2 for linear and rotational accelerations respectively. The maximum biases were approximately 1 g and 200 rad/s^2 for the on-field data. Uncertainties also varied with RME, with higher RME associated with higher uncertainties (Table 3.2). Maximum biases were found at the higher percentiles, with no apparent influence from sample size.

Table 3.2: Summary of the effects of changes in RME on uncertainties in descriptive statistics for the NFL (a) and on-field (b) data. Larger RME values were associated with larger uncertainties, though larger sample sizes were shown to mitigate this affect.

(a) NFL

		Linear Acceleration			Rotational Acceleration		
Percentile	Sample Size	Reduced RME (5.7%)	Published RME (11.4%)	Increased RME (17.1%)	Reduced RME (8.5%)	Published RME (17.5%)	Increased RME (25.5%)
50th	10	3.4%	5.8%	7.9%	4.6%	7.9%	10.8%
	100	1.5%	2.2%	2.8%	1.8%	2.8%	3.7%
	1000	0.5%	0.7%	0.9%	0.6%	0.9%	1.2%
95th	10	5.0%	9.1%	12.7%	7.2%	12.5%	17.2%
	100	2.2%	3.5%	4.6%	2.9%	4.6%	6.1%
	1000	0.8%	1.2%	1.5%	1.0%	1.5%	2.0%

(b) On-field

Percentile	Sample Size	Linear Acceleration Reduced RME (7.9%)	Linear Acceleration Published RME (15.7%)	Linear Acceleration Increased RME (23.6%)	Rotational Acceleration Reduced RME (15.9%)	Rotational Acceleration Published RME (31.7%)	Rotational Acceleration Increased RME (47.6%)
50th	10	4.8%	8.2%	11.1%	9.1%	15.8%	21.5%
	100	2.1%	3.1%	4.0%	3.7%	5.7%	7.5%
	1000	0.7%	1.0%	1.3%	1.2%	1.8%	2.4%
95th	10	7.5%	14.0%	19.8%	14.2%	25.5%	34.9%
	100	4.0%	6.5%	8.3%	6.5%	10.0%	13.1%
	1000	1.6%	2.3%	2.9%	2.3%	3.3%	4.3%

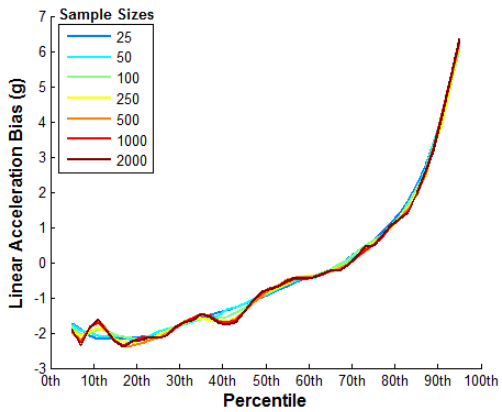

(a) NFL Linear Acceleration Bias

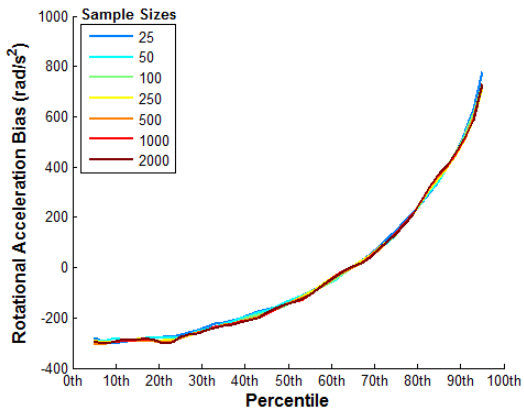

(b) NFL Rotational Acceleration Bias

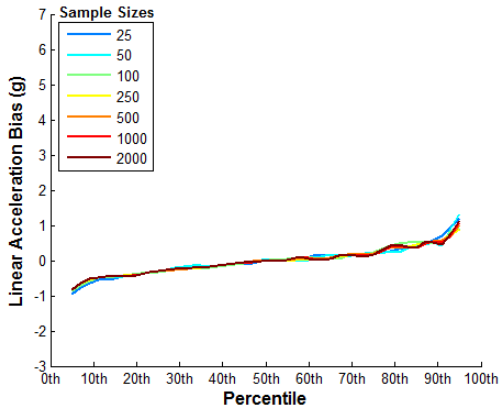

(c) On-field Linear Acceleration Bias

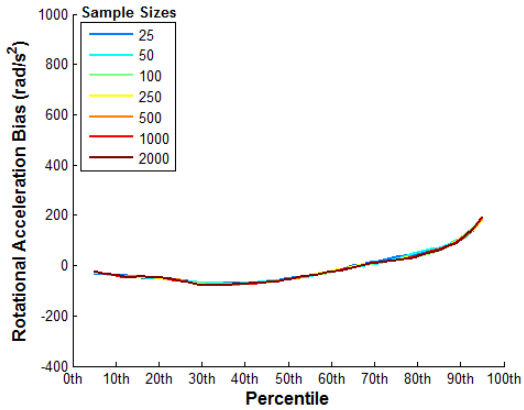

(d) On-field Rotational Acceleration Bias

Figure 3.5: Bias in linear (left) and rotational (right) acceleration percentiles for the NFL (top) and on-field (bottom) data for sample sizes ranging from 25 to 2000 samples. Maximum biases were found at the higher percentiles, with no apparent influence from sample size.

Analysis of Multiple Distributions

Team size was found to effect descriptive statistic uncertainty, with larger teams being associated with lower uncertainties (Figure 3.6). Using the published measurement error estimate, the 95th percentile linear acceleration uncertainties ranged from 4.2% to 0.9% and rotational accelerations ranged from 6.5% to 1.5% for team sizes of 2 to 200 players. Uncertainty estimates were also made for higher and lower RME values (Table 3.3). Bias was found to be primarily a function of percentiles and not of sample or team size.

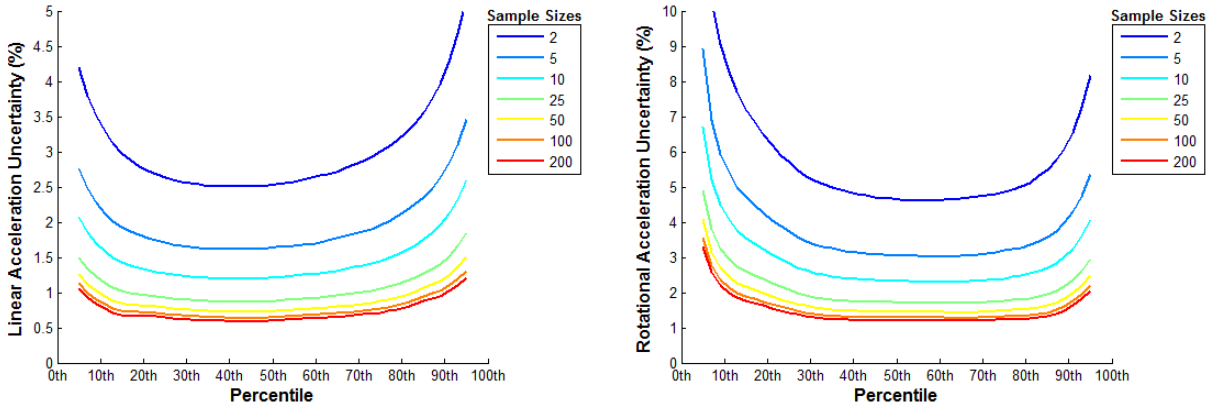

Figure 3.6: Average uncertainty in team descriptive statistics for linear (left) and rotational (right) accelerations for the on-field data with team sizes ranging from 2 to 200 players. Larger team sizes were associated with lower uncertainties.

Table 3.3: Average uncertainties in team descriptive statistics for linear and rotational accelerations for different RME values. While higher RME values were associated with higher uncertainties, larger sample sizes led to smaller uncertainties.

		Linear Acceleration			Rotational Acceleration		
Percentile	Team Size	Reduced RME (7.9%)	Published RME (15.7%)	Increased RME (23.6%)	Reduced RME (15.9%)	Published RME (31.7%)	Increased RME (47.6%)
50th	2	1.3%	2.0%	2.5%	2.3%	3.6%	4.6%
	10	0.6%	1.0%	1.2%	1.1%	1.8%	2.3%
	100	0.3%	0.5%	0.7%	0.6%	0.9%	1.2%
95th	2	2.6%	4.2%	5.4%	4.1%	6.5%	8.2%
	10	1.3%	2.1%	2.6%	2.1%	3.1%	4.0%
	100	0.6%	1.0%	1.3%	1.0%	1.7%	2.1%

Discussion

For the full dataset analyses, the uncertainties in descriptive statistics were lower than the random measurement error (RME) of individual data points for both the NFL and on-field sets. In general, the influence of RME was mitigated by the tendency of the RME from one data point to be neutralized by that of neighboring points. With more data points, there is a higher probability the RME of each data point is offset by that of other points. The on-field dataset, which is made up of over 4000 data points, had substantially lower uncertainties than the NFL dataset due largely to the difference in sample size. In Figure 3.3, there are differences in concavity among the three NFL dataset linear and rotational acceleration uncertainty curves and the curves are not as smooth as those of the youth dataset. These differences were due to the limited number of data points in the NFL dataset.

Sample size analyses demonstrated a clear trend of decreasing uncertainties with increasing sample size. As expected, greater numbers of data points were associated with less variation among

sample sets, leading to lower descriptive statistic uncertainties. Previous studies have found that football players average from around 100 head impacts per season at the youth level (ages 6-8 years) to 1000 impacts at the collegiate level.[16, 21, 46, 49] These average values corresponded to 50th and 95th percentile linear acceleration uncertainties of around 5% and 6% respectively for individual youth players and 1% and 2% for individual college football players. Impact totals are commonly split into smaller groups for categorical comparisons such as impact location or session type, resulting in smaller sample sizes. Researchers should be cognizant of the effect of small sample sizes when stratifying datasets or working with small datasets. In Figure 3.4, the uncertainty curves for the smaller sample sizes are not as smooth as those of larger sample sizes. The difference was particularly notable above the 70th percentile of the on-field dataset for a sample size of 25, where data points were especially sparse due to the small sample size and the elongated tail region of the distributions.

Averaging individual player descriptive statistics to produce team values was shown to reduce uncertainties further. The uncertainties for the team descriptive statistics are lower than those of individual players because they rely on data from multiple players, thus reducing the influence of random variations among players. Assuming all players on a particular team come from the same population, averaged data from more players will result in more accurate approximations of the true population averages. Typical youth football teams have around 15 to 25 players, corresponding to 95th percentile linear acceleration uncertainties under 2%, whereas college teams often have over 100, leading to uncertainties under 1%.

Bias is not substantially affected by sample size or team averaging. Rather, bias was primarily dependent on RME and percentile. Central percentiles, those around the 50th, are least affected by RME while those at the extremes are most affected. Larger RME led to an increase in data dispersion, leading to over prediction of 95th percentile values and under prediction of 5th percentile values. These biases were due to a higher probability of points moving away from the center than toward because of the distribution shape. For the NFL dataset, the 95th percentile linear acceleration was approximately 6 g. The 95th percentile linear accelerations were over estimated by approximately 1 g for the on-field dataset, with little variation among players. This difference was primarily due to the larger value of the NFL dataset 95th percentile acceleration compared to that of the youth, 135 g versus 47 g.

The uncertainty estimates presented in this study are intended to be representative of average conditions. Uncertainty ranges and median values are presented for select descriptive statistics for the actual football players from the on-field study along with the uncertainties in team statistical values (Table 3.4). Even in the case of maximum values, the estimated uncertainties are less than the RME of individual data points.

Table 3.4: Uncertainty estimates for descriptive statistics of the actual players from the on-field football study. Estimates were made for both linear and rotational accelerations for two commonly used descriptive statistics, the 50th and 95th percentiles.

		Linear Acceleration			Rotational Acceleration		
Percentile	Team Size	Reduced RME (7.9%)	Published RME (15.7%)	Increased RME (23.6%)	Reduced RME (15.9%)	Published RME (31.7%)	Increased RME (47.6%)
50th	2	1.3%	2.0%	2.5%	2.3%	3.6%	4.6%
	10	0.6%	1.0%	1.2%	1.1%	1.8%	2.3%
	100	0.3%	0.5%	0.7%	0.6%	0.9%	1.2%
95th	2	2.6%	4.2%	5.4%	4.1%	6.5%	8.2%
	10	1.3%	2.1%	2.6%	2.1%	3.1%	4.0%
	100	0.6%	1.0%	1.3%	1.0%	1.7%	2.1%

While RME in biomechanical data collected in the field may be higher than that of data collected in the laboratory, descriptive statistics of distributions typically have lower uncertainties than the individual data points that make up the set. A greater number of data points tends to leads to a greater reduction in descriptive statistic uncertainty compared with individual points. In the case of measuring head impact kinematics in football, instrumentation that can be worn on the field can provide large datasets over the course of a season. Distribution analysis techniques can then be used to offset the effects of RME. However, this is contingent on knowing the error of a given sensor or technique.

Field data is commonly used in other areas of sports and injury biomechanics, with RMEs often topping 10%. Automotive crash reconstruction software used by researchers in injury biomechanics has been shown contribute approximately 23% error to vehicle change of velocity (delta-v) estimates.[57] In exercise and sports biomechanics, where instrumentation is often custom-made, sensors and video are commonly used to collect data such as joint positions, reaction forces,

velocities and accelerations in the field and similar affects due to measurement errors have been noted, with measurement errors of around 10-30%.[58-61] Some laboratory instrumentation such as bands used to measure dynamic chest deflection in crash tests also have measurement errors on the scale of those found in TBI field studies, approximately 10%. [62] The uncertainty and bias analyses used in this study can be applied to the design and analysis of experiments that that involve data with non-negligible RME.

The Monte Carlo method presented here does introduce certain limitations to this study. RME, in addition to the RME that was inherent to the dataset, was added to the data in order to estimate the probability of various outcomes resulting in some estimate error. For the on-field data, the Monte Carlo method resulted in a small over estimation of peak linear and rotational acceleration uncertainties of 0.2 g and 15 rad/s^2. Uncertainty estimates of lower percentiles were less affected by the Monte Carlo analysis. Furthermore, inputs for this method, including RME estimates, were taken from previously published validation studies that have their own underlying limitations. Uncertainty and bias effects were quantified for several levels of RME to account for this limitation. The HIT System data presented in this study were from on-field football players so the uncertainty and bias estimates may not apply directly to adult data. Adult football players tend to sustain more impacts and impacts of higher magnitudes. The effect of these differences would lead to a slight increase in bias at the higher percentile levels but a lower uncertainty.

Biomechanical data collected in the field offer a high level of biofidelity that is generally not possible in the laboratory. Researchers should be mindful of the limitations of this data, however, as field data can be subject to higher random measurement error (RME) than data collected in the

laboratory. The analyses presented in this study have demonstrated how RME affects descriptive statistics when distribution analysis methods are applied. While individual data points may have relatively high measurement error, summary statistics from distributions of data are associated with reduced uncertainties.

Chapter 4: Quantitative Comparison of Hybrid III and NOCSAE Headform Shape Characteristics and Implications on Football Helmet Fit

Abstract

Laboratory tests which use dummy headforms to evaluate helmet performance must be representative of real-world conditions to ensure helmets perform well in the field. The objective of this study was to quantify shape differences that may affect helmet fit between two dummy headforms commonly used for football helmet testing. Point-cloud models of a 50th percentile male Hybrid III headform and medium NOCSAE headform were generated using a coordinate measuring machine. The headforms were optimally aligned and shape comparisons were made in the mid-sagittal plane, three coronal planes, and 3D. One coronal plane intersected the origin, while the other two were located anterior and posterior to the origin respectively. Planar and 3D differences were quantified by comparing maximum (*MRD*) and root-mean-square (*RMSD*) radial deviations. Minor differences were observed in the upper skull contours of all planar cross-sections. The *MRDs* ranged from 2.1 mm to 3.5 mm and *RMSDs* ranged from 1.1 mm to 1.7 mm while the 3D comparison yielded a *MRD* of 5.6 mm and *RMSD* of 1.4 mm. Larger deviations were observed in other regions including the jaw in the anterior coronal plane, where the *MRD* was 6.6 mm and *RMSD* deviation was 4.5 mm. Substantial differences were noted between the Hybrid III and NOCSAE at the base of the skull, cheeks, jaw and chin. The headforms were also compared to a head model based on medical imaging of a human subject. The NOCSAE was found to offer a better representation of the live subject in the regions where major differences were found

between the Hybrid III and NOCSAE. The data presented in this study show that the Hybrid III and NOCSAE headforms have substantial shape differences in several regions that are important for helmet fit which may make the NOCSAE a better option for realistic helmet fit.

Introduction

Laboratory tests in which helmeted dummy headforms are impacted in order to evaluate helmet performance must be representative of real-world conditions to ensure helmets perform well in the field.[10, 63, 64] Manufacturers design helmets to perform well in these laboratory tests, assuming the results translate to the field and lead to reduced head injury risk by reducing head acceleration.[13, 48, 49] Several types of headforms are used in the field of injury biomechanics for various testing applications including half headforms (ISO), automotive (Hybrid III), and full featured (Military, NOCSAE, FOCUS, custom).[44, 65-73] This study focused on shape comparisons between the most commonly used headforms in football helmet testing, the Hybrid III headform and the National Operating Committee on Standards for Athletic Equipment (NOCSAE) headform (Figure 4.1).[36, 38, 56, 74-84] While headform shape likely affects helmet fit and performance, morphological differences between these two headforms have not previously been quantified.

The Hybrid III headform was originally designed by General Motors in the 1970s as part of the ATD 502 crash test dummy for automotive safety testing.[85] Later, a more advanced crash test dummy, the Hybrid III, was developed and the ATD 502 headform was carried over to the new dummy.[73] Gross anthropomorphic measurements, facial landmarks, and inertial properties were selected for the headform to represent the average American man.[73, 86, 87] In addition, the biomechanical response of the headform was tested to ensure reasonable biofidelity for both direct

loading from impacts to the head and loading through the neck attachment at the occipital condyle.[85] The Hybrid III headform is commonly selected for helmeted head impact studies in which a model that includes a biofidelic neck or full dummy body is used.[28, 38, 82]

Figure 4.1: The Hybrid III (left) and NOCSAE (right) headforms are the most commonly used headforms in helmet impact performance testing.

Around the same time the Hybrid III headform was in development, researchers were working on a dummy head for testing athletic helmets, commonly known as the NOCSAE headform.[71] The NOCSAE headform was designed specifically for conducting drop tower tests for football helmets. Size and shape specifications for the headform were based on a cadaver head which researchers identified as being representative of an average adult football player's head. Researchers opted to include the upper part of the neck with the headform by which it is rigidly attached to the test apparatus. The skull deflection properties of the headform were tested to ensure conformity with cadaver models.[71] Researchers typically select the NOCSAE headform for head impact studies in

which a rigidly attached headform is used. Custom modifications can be made to the headform, however, that allow for attachment to a Hybrid III neck.[10, 79, 81, 82]

Headform shape can affect helmet fit which may alter helmet impact performance in laboratory tests. The objective of this study was to quantify shape differences between two dummy headforms commonly used for football helmet testing, Hybrid III and NOCSAE, emphasizing how differences may affect helmet fit.

Materials & Methods

The 50th percentile male Hybrid III and medium NOCSAE headforms, were scanned using a coordinate measuring machine equipped with a Laser ScanArm (FARO, Lake Mary, FL), capable of a measurement accuracy of ± 35 μm. Position data for points on the surfaces of the two headforms were collected and used to generate 3D point-cloud representations. For scanning, the headforms were mounted to a 50th percentile male Hybrid III neck which was rigidly mounted to a table. Post processing of the 3D data to remove excess points and smooth surfaces was conducted using Geomagic Studio 2012 software (3D Systems, Rock Hill, SC). The resulting point-cloud data were imported into MATLAB (MathWorks, Natick, MA) for dimensional analyses.

MATLAB script files were written to import the point-cloud data using the Wavefront OBJ toolbox [88] and to align the headforms to a common global coordinate system. The mid-sagittal plane of each headform was found by comparing symmetry across the mid-lines of three coronal

plane cross-sections: one 38.1 mm (1.5 in) anterior to the center of gravity (CG) of the headform, a second at the CG, and a third 63.5 mm (2.5 in) posterior to the CG. Each coronal cross-section was divided into 1˚ increments from -90˚ to 90˚ with the 0˚ line at the top of the headform, separating the left and right sides. The root-sum-square (*RSS*) of differences between corresponding radius values on the left and right sides (Equation 4.1) were determined for each coronal plane as roll (lateral neck flexion) and yaw (head rotation about the long axis of the body) of the head were varied.

$$RSS_{L-R} = \sqrt{\sum_i \left(r_R(\theta_i) - r_L(-\theta_i)\right)^2} \tag{4.1}$$

The first term in Equation 4.1 corresponds to the radii on right (*R*) side and the second term to those on the left (*L*) side of the head with the angle (ϑ_i) ranging from 1˚ to 90˚. The head orientation where the sum of the *RSS* values from the three coronal planes was minimized was selected as the mid-sagittal plane of the headform. After defining the mid-sagittal plane for each headform, the headforms were aligned to a common coordinate system about the CG of the Hybrid III. The RSS of the differences between the Hybrid III and NOCSAE headforms in the mid-sagittal plane (Equation 4.2) were minimized by varying pitch angle (neck flexion/extension) of the NOCSAE and translating it in the sagittal plane.

$$RSS_{HIII-NOCSAE} = \sqrt{\sum_i \left(r_{HIII}(\theta_i) - r_{NOCSAE}(\theta_i)\right)^2} \tag{4.2}$$

The first term in Equation 4.2 represents the radii of the Hybrid III for each angle, θ, in the plane of interest and the second term represents those of the NOCSAE for θ_i values ranging from -15˚

to 145˚. In the mid-sagittal plane, the polar coordinate system ranged from -180˚ to 180˚ with 0˚ at the back of the headform and ±180˚ at the front with positive angles measured counterclockwise.

Once the headforms were aligned, comparisons were made between headforms in four planes of interest and in 3D. Cross-sectional comparisons were made in the mid-sagittal, anterior-coronal (38.1 mm from the CG), mid-coronal (through Hybrid III CG), and posterior-coronal (63.5 mm from the CG) planes to highlight key differences between the headforms in regions that are likely to be in contact with helmet padding. The 3D comparison excluded regions that were unlikely to affect helmet fit, such as the face, ears, and areas below the bottom edge of a helmet.

For the cross-sectional comparisons, the data were transformed from Cartesian to a polar coordinate system in the planes of interest. Two metrics were used to quantify differences in the cross-sectional planes: root-mean-square radial deviation (*RMSD*) and maximum radial deviation (*MRD*). The *RMSD* was defined by Equation 4.3, where *N* is the number of points compared. The MRD was defined by Equation 4.4.

$$RMS = \sqrt{\frac{1}{N}\sum_{i}\left(r_{HIII}(\theta_i) - r_{NOCSAE}(\theta_i)\right)^2} \tag{4.3}$$

$$MRD = \left(r_{HIII}(\theta_i) - r_{NOCSAE}(\theta_i)\right)_{max} \tag{4.4}$$

The ranges over which the two headforms were compared in each plane were selected to represent regions where a football helmet is likely to contact the head (Table 4.1). Ranges where the headforms deviated substantially from one another were excluded from *RMSD* and *MRD*

calculations, but were highlighted and discussed separately. The included ranges were selected such that the *MRD* was not at the edge of the range. For the mid-sagittal contour, the polar coordinate system ranged from -180˚ to 180˚ with 0˚ at the right side of the figures (along the positive x-axis). For all three coronal contours, the coordinate system ranged from -180˚ to 180˚ with 0˚ at the top of the figures.

The same metrics, *RMSD* and *MRD*, were used for 3D comparisons. A spherical coordinate system was defined, with the origin located at the CG of the Hybrid III. Azimuth ranged from -180˚ to 180˚ with 0˚ at the front of the headform and positive values on the left side. Elevation ranged from -90˚ to 90˚ with negative at the bottom, positive at the top, and 0˚ passing through the origin. Comparisons between the headforms were made at 1˚ increments of azimuth and elevation for all azimuth values and elevation values greater than -30˚ (Figure 4.2). Regions which were unlikely to affect helmet fit were excluded. In the face region, where azimuth values range from -45˚ to 45˚, elevation values below 20˚ were excluded. Likewise, the ear regions, -90˚ to -130˚ and 90˚ to 130˚, were excluded below an elevation of 15˚. On the back of the heads, where azimuth values ranged from -130˚ to -180˚ and 130˚ to 180˚, elevation values below -15˚ were excluded. The ear and face regions are not expected to substantially impact helmet fit or performance. The differences at the base of the headforms, which are likely to have an effect on helmet fit, will be discussed separately.

Table 4.1: Ranges over which planar comparisons were made among headforms. The ranges were selected to make comparisons between headforms in regions relevant to football helmet fit.

Plane	Headform Comparison Regions		
Mid-Sagittal	Upper skull -15˚ to 155˚	Base of skull -15˚ to -35˚	Chin -120˚ to -135˚
Mid-Coronal	Upper skull -100˚ to 100˚	Left Jaw -100˚ to -145˚	Right Jaw 100˚ to 145˚
Anterior-Coronal	Upper Skull -115˚ to 115˚	Left Jaw -115˚ to -155˚	Right Jaw 115˚ to 155˚
Posterior-Coronal	Upper skull -115˚ to 115˚	Lower Left -115˚ to -145˚	Lower Right 115˚ to 145˚

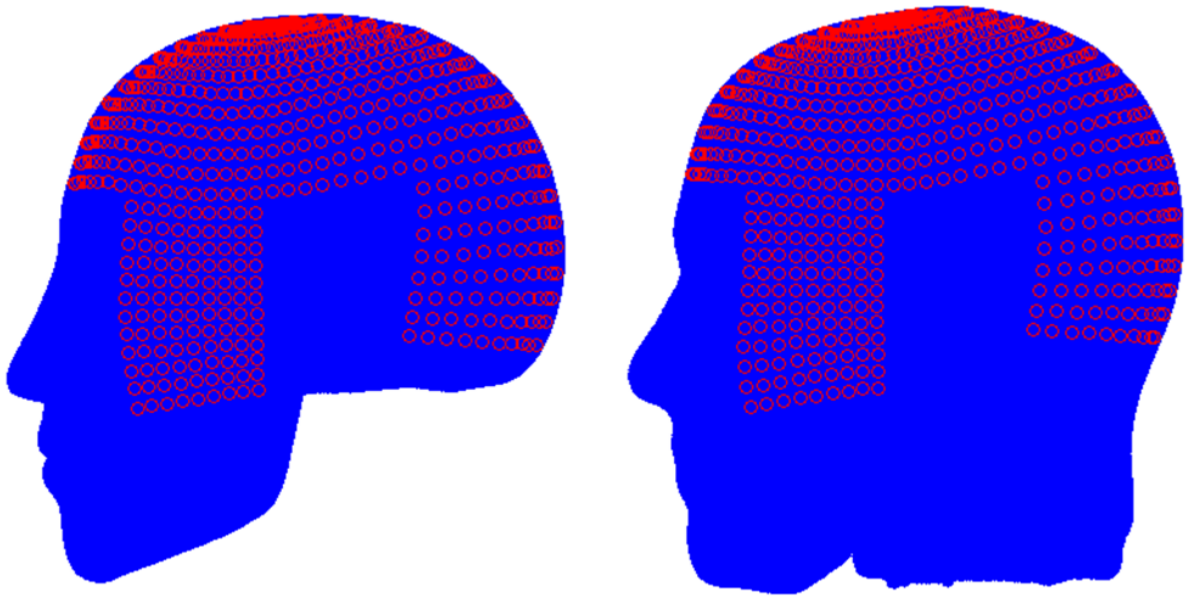

Figure 4.2: Profile view of the (a) Hybrid III and (b) NOCSAE headforms with markers indicating the locations of 3D comparative radial measurements between the two headforms. Circle locations were defined in spherical coordinates by azimuth and elevation at 1˚ increments.

Results

In the mid-sagittal contour, the upper skull regions, which go from the base of the skull to the brow (-15˚ to 155˚), were nearly identical (Figure 4.3). The *MRD* between the two headform in this

region was found to be 2.1 mm, located on the forehead. The *RMSD* over this range was 1.1 mm. More substantial differences were evident around the base of the skull (-15˚ to -35˚) where the contours of the two headforms diverge. The Hybrid III contour follows the shape of the occipital bone while the NOCSAE contour continues down, following the shape of the neck. One more notable difference between headforms that was evident in this plane was the difference in chin shape (-120˚ to -135˚). Comparing the chins between the two headforms, a *MRD* of 7.6 mm and *RMSD* of 3.4 mm were found. Some minor differences were found in the remaining facial region but they are not likely affect helmet fit.

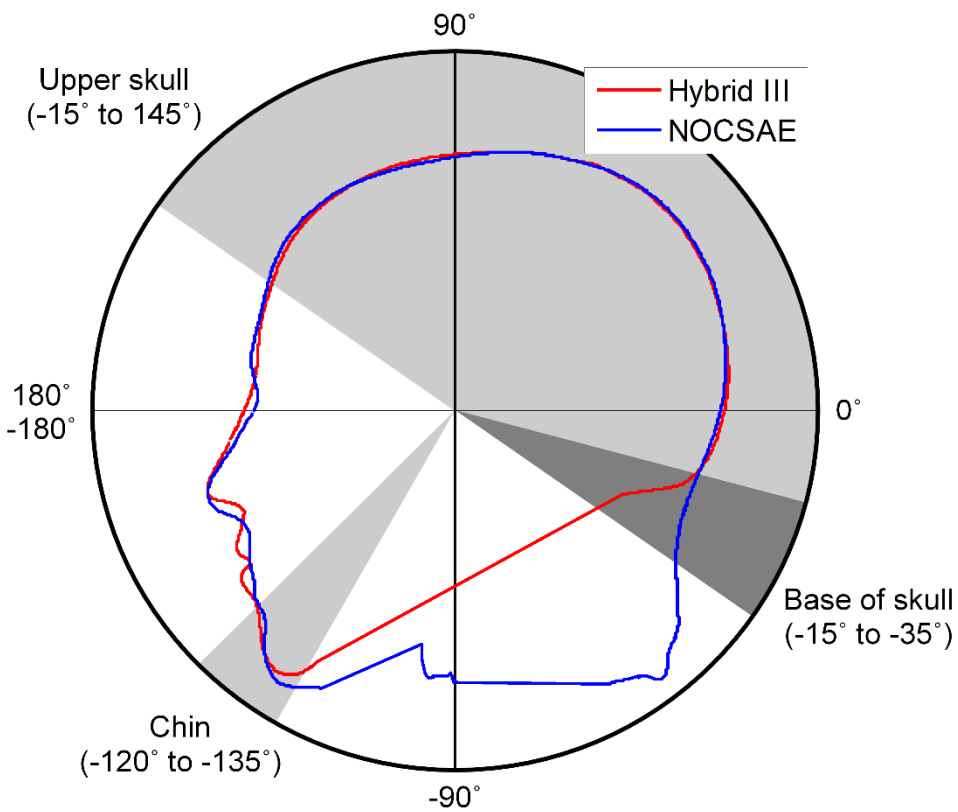

Figure 4.3: Mid-sagittal plane cross-section of Hybrid III (red) and NOCSAE (blue) headforms. Along the upper portion of the skull, the *MRD* was 2.1 mm and *RMSD* was 1.1 mm. The deviations at the base of the skull and chin are more substantial.

At an offset of 38.1 mm (1.5 in) anterior to the CG of the Hybrid III (Figure 4.4), the differences between the two headforms in the jaw region which were noted in the mid-coronal plane become more pronounced. The *MRD* in the lower portion of this cross-section (-115˚ to -155˚ and 115˚ to 155˚ on the left and right respectively) was 6.5 mm and the *RMSD* was 4.6 mm. The upper portion has a *MRD* of 3.5 mm and *RMSD* of 1.7 mm.

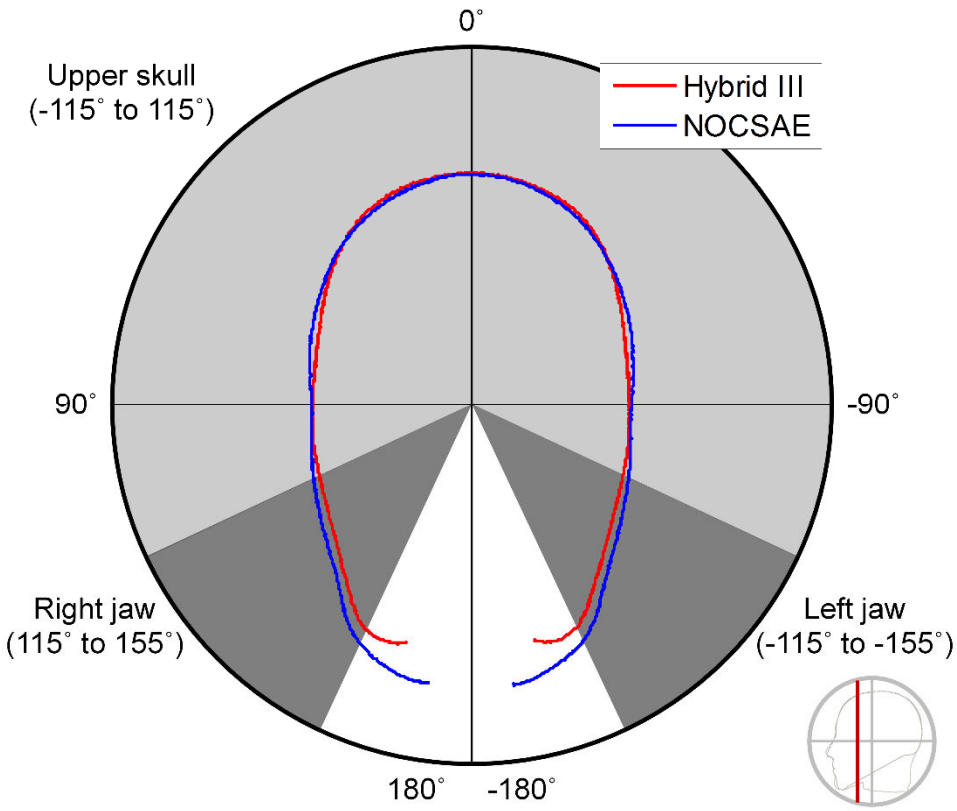

Figure 4.4: Coronal plane cross-section of a Hybrid III (blue) and NOCSAE headform through a point 38.1 mm (1.5 in) anterior to the CG of the Hybrid III. Along the upper portion, the *MRD* was 3.5 mm and the *RMS*D was 1.7 mm. At the jaw, the values were 6.5 mm and 4.6 mm respectively.

The two headforms were also nearly identical in the upper skull region (-100˚ to 100˚) of the coronal plan passing through the CG of the Hybrid III (Figure 4.5). The *MRD* between the two headforms was found to be 2.1 mm while the *RMSD* was 1.2 mm. In the lower portions of the headforms (-100˚ to -145˚ and 100˚ to 145˚ on the left and right respectively), where the contour cuts through the jaw, the Hybrid III is noticeably narrower than the NOCSAE. The *MRD* between the two headforms in this region was 7.6 mm and the *RMSD* was 4.2 mm. In addition to being narrower, the Hybrid III headform does not extend as far down as the NOCSAE.

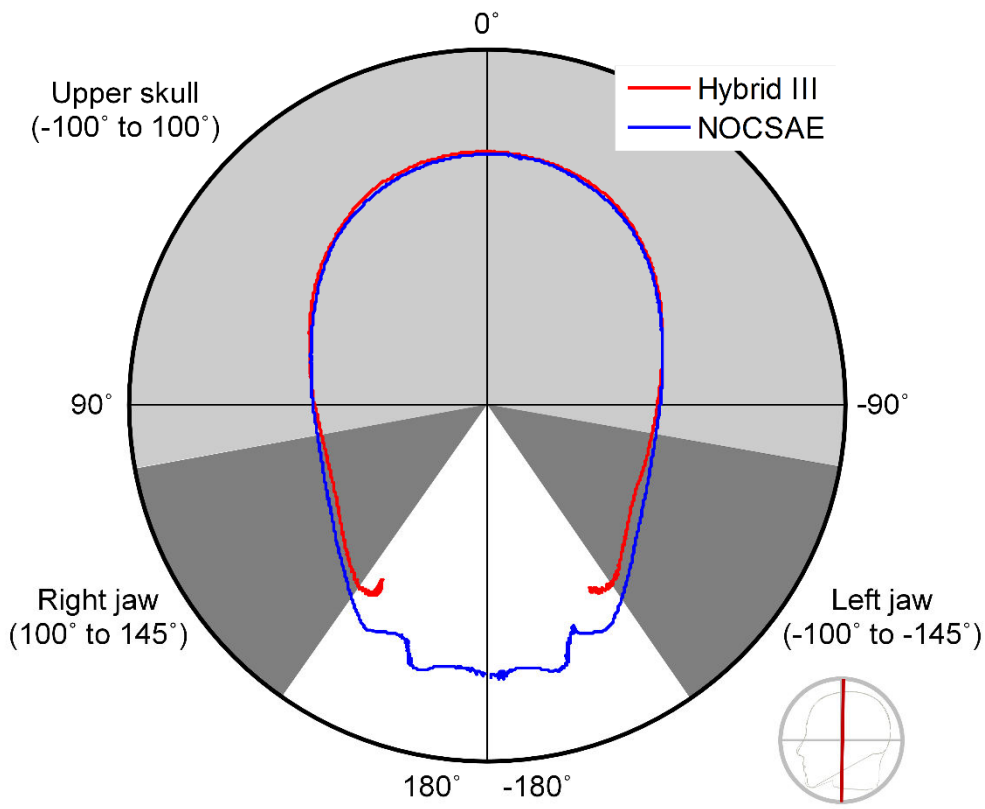

Figure 4.5: Coronal plane cross-section of the Hybrid III (red) and NOCSAE (blue) headform through the CG of the Hybrid III. The MRD along the upper skull was 2.1 mm and the *RMSD* was 1.2 mm. At the jaw, the values were 7.6 mm and 4.2 mm respectively.

Differences between the two headforms were more apparent 63.5 mm (2.5 in) posterior to the CG (Figure 4.6). The upper portions of the headforms (-115˚ to 115˚) still matched well, with a *MRD* of 2.6 mm and *RMSD* of 1.4 mm. A more substantial difference was evident in the lower portion of the headforms, where the two contours diverge. Similar to the mid-sagittal plane, the contour of the Hybrid III resembles the shape of the skull only, but the NOCSAE contour includes the upper part of the neck. The regions of divergence are highlighted in Figure 6 from -115˚ to -145˚ and 115˚ to 145˚.

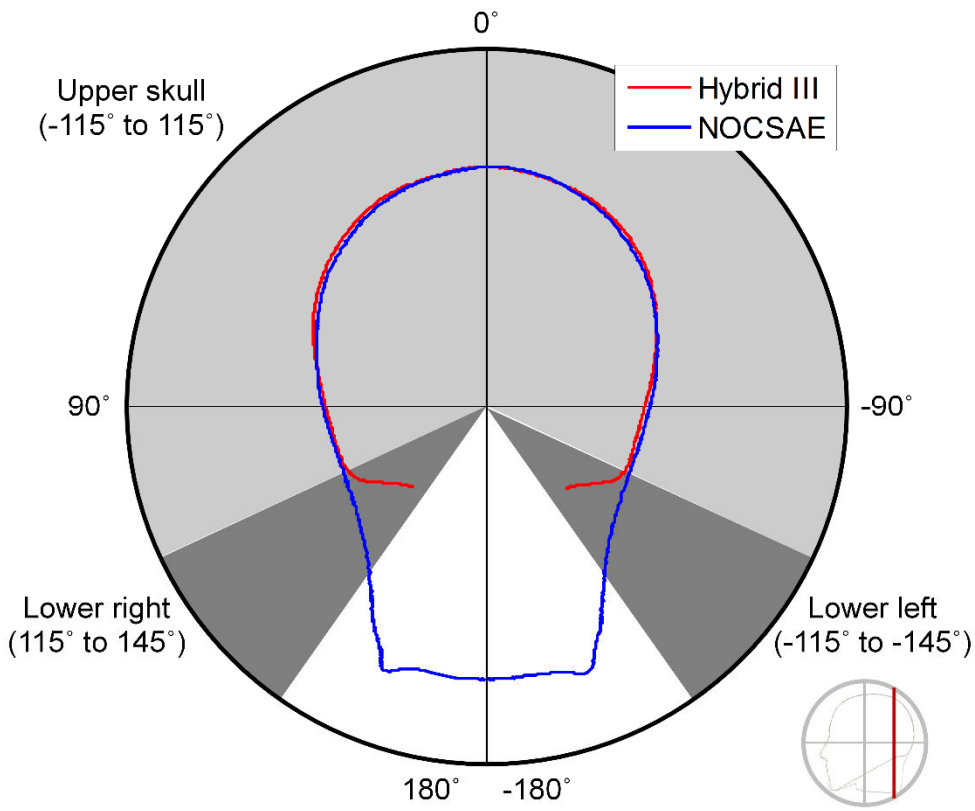

Figure 4.6: Coronal plane cross-section of the Hybrid III (red) and NOCSAE (blue) headform through a point 63.5 mm (2.5 in) posterior to the CG of the Hybrid III. Along the upper skull, the *MRD* was 2.6 mm and was *RMSD* 1.4 mm. For the lower portions of the contour, the headforms deviate substantially.

For the 3D comparisons, the differences between the headforms were minor in most regions (Figure 4.7). The *MRD* was 5.6 mm and the *RMSD* was 1.4 mm. The largest deviations between the headforms occurred in the cheek and jaw regions.

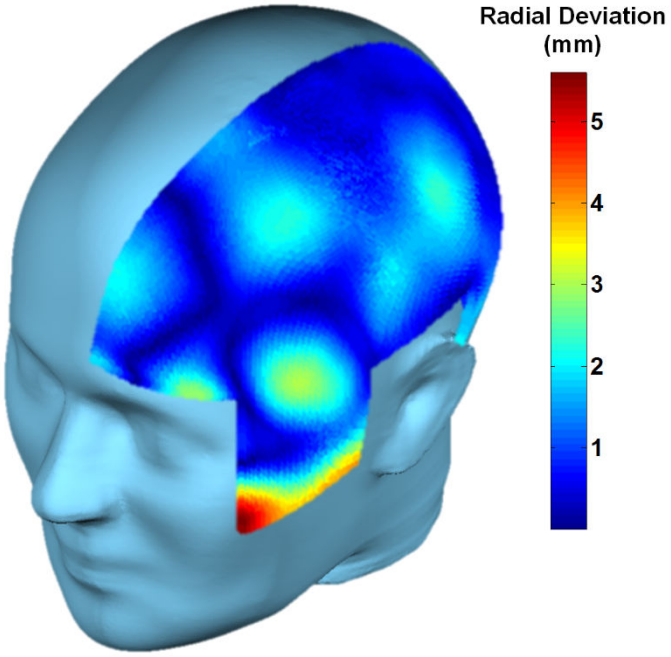

Figure 4.7: Heat map showing the 3D comparison between the Hybrid III and NOCSAE headforms displayed on a NOCSAE headform. The differences on the right and left sides were averaged and displayed on the left side of the headform. The largest radial deviations, those greater than 3.5 mm, occurred in the cheek region of the headforms and are indicated by orange and red coloration in the figure.

Discussion

Headform shape affects helmet fit during laboratory testing of football helmets. Laboratory tests provide manufacturers and consumers with an objective measure of a helmets ability to reduce head acceleration due to direct impact. In order for test results to translate into reduced injury risk

in the field however, the tests must be representative of real life conditions, including helmet fit. Helmet-head coupling may play an important role in football helmet performance in the field. Padding in the helmet must make contact with the head in order to be compressed and dissipate impact energy. In the upper portion of the headforms, only minor differences were found. The differences are unlikely to substantially affect helmet fit as padding will deform to accommodate the minor variations in head shape. Differences in the base of the skull, the jaw, and the cheeks explain the issue of fitting a helmet to the Hybrid III. The padding should be in contact with the head in these three regions making them important for quality of helmet fit and performance. Differences between the chins of the two headforms may affect chinstrap fit and performance.

The Hybrid III headform does not contact the helmet padding at the bottom edge of many helmets because it does not extend down far enough at the base of the skull (Figure 4.8). The NOCSAE headform, which includes the upper part of the neck, does extend below the bottom edge of helmets and contact the padding in this region. During rear impacts, the impact loading on the Hybrid III headform may tend to be more concentrated, potentially altering the effective stiffness of the helmet padding and helmet performance. Furthermore, impacts in some locations, such as those near the bottom of the helmet shell, may induce helmet rotation with respect to the Hybrid III headform which may also affect helmet performance in addition to test repeatability.

Figure 4.8: Left profile view of a Hybrid III (left) and NOCSAE headform inside a cross-sectioned football helmet. At the base of the helmet, the Hybrid III headform does not contact the padding whereas the NOCSAE does.

Modern football helmets are also designed with padding meant to contact the face around the cheek bones and jaw. This padding, in addition to the forehead padding, absorbs energy from impacts to the front of the helmet shell and facemask. Figure 4.4 illustrates the differences between the Hybrid III and NOCSAE headforms in the cheek bone and jaw regions. The Hybrid III headform is narrower, leaving a larger gap between the headform and helmet padding. The larger gap allows for greater helmet rotation relative to the headform during frontal and side impacts, which is not characteristic of proper helmet fit. Impacts to the lower portion of the facemask are especially prone to cause helmet rotation on the Hybrid III due to the gap between the padding and the

headform in the cheek bone and jaw regions. Both standard and extra-thick jaw pads leave a gap between the Hybrid III headform and the padding in most helmets.

The two headforms were also compared to the head of a human body model, the 50th percentile male Global Human Body Models Consortium (GHBMC) model, which was developed using medical imaging of a live human subject (Table 4.2). [89] This model is a part of an ongoing project involving several automotive companies to develop more realistic and robust human body models to more accurately represent real-world injury conditions with computational methods and advance crash safety technology. Both headforms show good agreement with the GHBMC head in the upper skull region though the headforms matched each other more closely than either matched the GHBMC. Comparisons in the three coronal planes yielded similar results for the upper skull regions. At the base of the skull, where the Hybrid III and NOCSAE headforms differ, the GHBMC more closely resembles the shape of the NOCSAE headform. In the jaw region of the anterior coronal plane, the GHBMC jaw is wider than that of either the Hybrid III or NOCSAE headform. The NOCSAE jaw, which is wider than that of the Hybrid III, offers a closer match to the GHBMC model. While the NOCSAE headform offers a better representation than the Hybrid III of the GHBMC head, it should be noted that both the NOCSAE headform and GHBMC model were based on anthropomorphic measurements from single human subjects thought to be representative of the 50th percentile male and do not account for variations in head shape between human subjects.

Table 4.2: Comparison of the Hybrid III and NOCSAE headforms with the GHBMC head in various cross-sectional planes. Larger differences were found between the Hybrid III and GHBMC than the NOCSAE and GHBMC for both maximum radial deviation (*MRD*) and RMS radial Deviation (*RMSD*) in most regions.

		Maximum Radial Deviation (mm)		RMS Radial Deviation (mm)	
Plane	Region	Hybrid III vs. GHBMC	NOCSAE vs. GHBMC	Hybrid III vs. GHBMC	NOCSAE vs. GHBMC
Mid-Sagittal	Upper Skull	4.7	4.4	2.0	2.4
	Chin	11.6	5.5	4.9	2.8
Anterior-Coronal	Upper Skull	5.0	3.8	1.6	1.8
	Jaw	10.6	6.3	7.9	3.9
Mid-Coronal	Upper Skull	8.7	7.0	3.5	3.4
	Jaw	18.3	13.0	14.7	10.7
Posterior-Coronal	Upper Skull	10.8	9.2	4.9	4.7

In frontal impacts, the chinstrap helps to keep the helmet in place and transfer energy to the helmet to be dissipated. Impacts to the facemask, especially those low on the facemask, tend to cause the helmet to rotate relative to the head. Chin shape may affect the performance of the chinstrap, which counteracts forces that tend to cause helmet rotation. On the Hybrid III headform, the chin is more pointed and does not protrude as far forward as that of the NOCSAE. The chin on the Hybrid III, which was not designed to accommodate a chinstrap, provides a smaller moment arm for the chinstrap to counteract horizontal forces applied to the facemask that tend to rotate the helmet. The smaller moment arm may increase decoupling of the helmet and head during frontal impacts, altering the helmet padding's ability to dissipate energy. Future studies should investigate the effect of fit on helmet performance.

The differences in shape between the Hybrid III and NOCSAE headforms highlighted in this study make proper fitting of football helmets to the Hybrid III headform difficult. While the circumference of the headform suggests a Large helmet should be selected, that helmet size tends to move excessively relative to the headform, even with helmet bladders fully inflated.[90] In this case, the manufacturer supplied fit guides suggest using a smaller helmet. The shape of the medium NOCSAE headform allows for proper fit of a large helmet. Impact performance is likely affected by helmet fit though future studies are needed to quantify that affect. If helmet evaluation standards utilized a Hybrid III headform, manufacturers may alter the shape of their helmets to better accommodate this headform, leading to poorer helmet fit on real football players.

Several important limitations should be noted regarding this study. Only one headform of each type was measured in this study. Other Hybrid III and NOCSAE headforms which meet the respective manufacturing tolerances may yield slightly different measurements, though the differences are not expected to substantially affect the results or conclusions of this study. The analysis addressed only headform shape characteristics. Other factors such as inertial properties, attachment to a biofidelic neck, and instrumentation installation should also be considered in future studies. Measurements were taken of headforms that were intended to represent an average man, limiting the applicability of these results for large or small men, women, and children. Comparisons were made in regions important to football helmet fit so the conclusions may not be directly applicable to other types of helmets. The ear regions were excluded from the analysis because the NOCSAE headform has only one ear and the Hybrid III has none. This limitation is expected to have a minimal effect on helmet fit.

Proper helmet fit and sizing on dummy headforms for laboratory testing is dependent on headform shape. The head circumference measured above the brow alone is not adequate to characterize headform size for helmet testing. Football helmets also contact the nape of the neck, the jaw, and the cheek bones and are attached via a chinstrap. In this study, the differences in shape between the Hybrid III and NOCSAE headforms were quantified. While only minor differences were noted in the upper portions of the headforms, substantial differences were found in other areas. The jaw and cheeks were found to be narrower in the Hybrid III compared with the NOCSAE headform. In addition, the back of the Hybrid III headform does not extend all the way to the bottom edge of helmets. These differences may lead to reduced head-helmet padding surface area and likely allow for more helmet rotation relative to the headform, neither of which is representative of on-field head impacts.

Chapter 5: Comparative Analysis of Helmeted Impact Response of Hybrid III and NOCSAE Headforms

Abstract

As advanced helmet testing methodologies are developed, the affect headform selection may have on the biomechanical impact response must be considered. This study sought to assess response differences between two of the most commonly used headforms, the Hybrid III and NOCSAE headforms, through a series of helmeted impact tests. The two headforms, which were both mounted on a Hybrid III neck attached to a slider table, were impacted ninety times each using six locations and three velocities. Test condition-specific significant differences were found between the two headforms for peak linear and angular accelerations ($\alpha = 0.05$), though differences tended to be small. On average, the NOCSAE headform experienced higher peak linear (3.7 ± 7.8%) and angular (12.0 ± 21.6%) accelerations, with some of the largest differences associated with impacts to the facemask. Without the facemask impacts, the average differences in linear (1.8 ± 6.0%) and angular (9.6 ± 15.9%) acceleration would be lower. No significant differences were found in coefficient of variation values for linear (HIII: 2.6 ± 2.3%, NOCSAE: 2.0 ± 1.4%) or angular (HIII: 4.9 ± 4.0%; NOCSAE: 5.2 ± 5.8%) acceleration. These data have application toward development and validation of future helmet evaluation protocols and standards.

Introduction

Athletic helmets are evaluated for impact performance using laboratory tests with dummy headforms in an effort to assess brain injury risk.[10, 81] While various headforms are used in the field of injury biomechanics, the two most commonly used for evaluation of sports helmets are the Hybrid III and National Operating Committee on Standards for Athletic Equipment (NOCSAE) headforms.[10, 28, 38, 56, 74, 75, 78, 82, 91-93] Differences between these two headforms such as shape, instrumentation, materials, and inertial properties are likely to affect the measured kinematic response in helmeted impact tests.

Football helmet evaluation standards began in the 1970s when NOCSAE developed and implemented a drop tower testing methodology to improve helmet safety.[71] This drop tower test involves dropping a NOCSAE headform that is rigidly mounted to a twin wire-guided carriage onto an anvil. While this type of test can reproduce the sorts of linear accelerations observed in on-field head impacts, the rigid neck precludes a realistic angular acceleration response.[82] Angular head acceleration is widely believed to be an important factor in sports-related brain injury.[6, 11, 12, 94, 95] Other methodologies including pneumatic linear impactor and pendulum tests have been developed to more accurately represent on-field head impact responses in the laboratory.[79, 82] These types of tests involve a dummy headform mounted on a neck which produces a 3D kinematic head response that is more consistent with on-field data in terms of acceleration trace shape and duration than test conducted with a rigid attachment. Both the Hybrid III and NOCSAE headforms are commonly used in these other testing methodologies. In situations where a full dummy body is used, the Hybrid III is most often selected, though when only the neck and head are used, both

headforms are commonly chosen.[6, 7, 10, 12, 20, 21]While this study will focus on football helmet testing, the findings may be transferrable to other sports helmet evaluations.[69, 76, 96]

The Hybrid III headform is a part of the full-body anthropomorphic test device (ATD) by the same name. The dummy was designed for automotive safety testing by researchers working for General Motors. In addition to automotive safety, the Hybrid III headform has also been used extensively for sports helmet testing.[28, 29, 32, 78, 82, 85] The full body ATD includes a biofidelic neck to which the headform can be attached, allowing for angular accelerations.[78] A hollow cavity in the headform also makes it well suited for the instrumentation used to measure linear and angular head acceleration.[97] The biomechanical response of the head has been validated for direct loading and loading through the neck attachment.[85] While the dimensions and shape of the upper part of headform were based on measurements from a cadaver, the headform was not designed to evaluate head protection. Some portions of the headform are not representative of a human head making proper helmet fit difficult.[98]

Contrary to the Hybrid III, the NOCSAE headform was developed specifically for helmet testing.[71] The headform was built to replicate linear acceleration characteristics in drop tower tests; as such, the headform attaches rigidly to a drop carriage and has limited space for instrumentation. A shaft from the underside of the chin to an area near the center of gravity (CG) of the headform was designed to allow for placement of a triaxial accelerometer package for linear acceleration measurement only.[74] While previous studies have implemented other six degree of freedom (DOF) instrumentation arrangements, recent advances in instrumentation technology have also allowed

researchers to accurately measure 6DOF using an accelerometer and angular rate sensor package that fits inside the NOCSAE instrumentation shaft. Size and shape specifications for the headform were based on a cadaver determined to be representative of the average American football player and the model includes all parts of the head that are important for helmet fit.[71]

To date, no studies have compared impact response characteristics for Hybrid III and NOCSAE headforms where both heads were mounted on a Hybrid III neck. Differences between the two headforms in mass, inertia, instrumentation, and other properties are likely to have implications on impact test results. This study tested the hypothesis that there would be no difference in impact responses between the Hybrid III and NOCSAE headforms over a range of acceleration magnitudes that have been observed in the field.

Materials & Methods

Impact tests were conducted on two helmeted dummy headforms, a 50th percentile male Hybrid III and a medium NOCSAE headform (Figure 1). Both headforms were mounted on a 50th percentile male Hybrid III neck attached to a five degree of freedom (DOF) adjustable linear slide table which represented the effective mass of the torso.[7, 10] All tests were conducted using a custom pendulum impactor consisting of a 15.5 kg anvil with a flat impactor face at the end of a 1.90 m arm. The total moment of inertia of the pendulum arm and anvil was 72 kg-m^2. The impactor face was a 127 mm (5 in) diameter, 25 mm thick piece of nylon mounted directly to a steel anvil. The two headforms were fitted with a large Riddell Speed Revolution helmet (Riddell, Rosemont, IL), and struck five times at each test condition using six locations and three impactor velocities for a total of one hundred eighty tests. Impact locations on the front, facemask, jaw, side, rear boss, and

rear of the helmet (Figure 3) were selected to represent commonly impacted regions of the helmet and facemask based on previously published studies.[25, 28] For each impact location, the headforms were rotated into the same positions and then translated to align markers on the helmet with the impactor face. The slide table allows for rotations to lean the head and neck toward or away from the impactor (elevation) and twist the head and neck about the long axis of the body (azimuth). Impactor velocities of 3.1 m/s, 4.9 m/s, and 6.4 m/s were selected to reproduce a range of linear accelerations similar to those observed in on-field head impact datasets. The selected magnitudes roughly correspond to on-field impacts from the 95th percentile to the 99.9th percentile. [7, 9, 29-32] High magnitude impact conditions were selected for this study because they are the most likely to cause injury and therefore most relevant for evaluating brain injury risk in the laboratory.

Figure 5.1: The most commonly used headforms in helmet impact testing, (a) a 50th percentile male Hybrid III headform and (b) a medium NOCSAE headform, both mounted on a 50th percentile male Hybrid III neck.

Kinematic data of the Hybrid III headform were collected at 20 kHz using nine accelerometers (7264-2000B, Endevco, San Juan Capistrano, CA) in a 3-2-2-2 arrangement. The accelerometer arrangement allowed for calculation of linear and angular acceleration about the center of gravity of the headform. Linear acceleration data were filtered in accordance with SAE J211 standards using a Channel Frequency Class (CFC) 1000 low-pass anti-aliasing filter. Angular acceleration data were filtered with a CFC 180 filter for angular acceleration calculations in accordance with published best-practices to reduce the effect of spurious noise.[38, 56]

While the Hybrid III headform was mounted on the Hybrid III neck as designed, the NOCSAE headform required a custom adapter plate and modifications to the headform (Figure 2) to allow for neck attachment. The adapter plate mounted on the base of the headform via three screws that fit into existing threaded holes. A 12.7 mm (0.5 in) diameter shaft through the adapter plate allowed for attachment to a Hybrid III neck via the occipital condyle (OC) joint similar to how the Hybrid III headform attaches. The adapter plate was 22.2 mm (0.875 in) thick and the bottom face sat directly on top of the neck, without rubber nodding blocks (a standard feature on the Hybrid III neck). Minor modifications were made to the NOCSAE headform to accommodate the adapter plate and move the OC joint forward to more closely resemble relative position of the OC joint to the CG of the Hybrid III headform. The plate was placed such that the distance in the anterior-posterior and medial-lateral directions between the OC joint and the CG would be the same for the Hybrid III and NOCSAE headforms. With the adapter plate, the OC joint was 22 mm inferior of the CG than the OC joint on the Hybrid III headform. The OC joint shaft was centered 18.8 mm

(0.74 in) forward of center threaded hole in the headform and 12.7 mm (0.50 in) inferior to the base of the headform. Some material was removed from the headform around the original neck mount and instrumentation channel (Figure 2) to make room for the adapter plate and Hybrid III neck. The mass of the adapter plate and mounting screws matched that of the removed material.

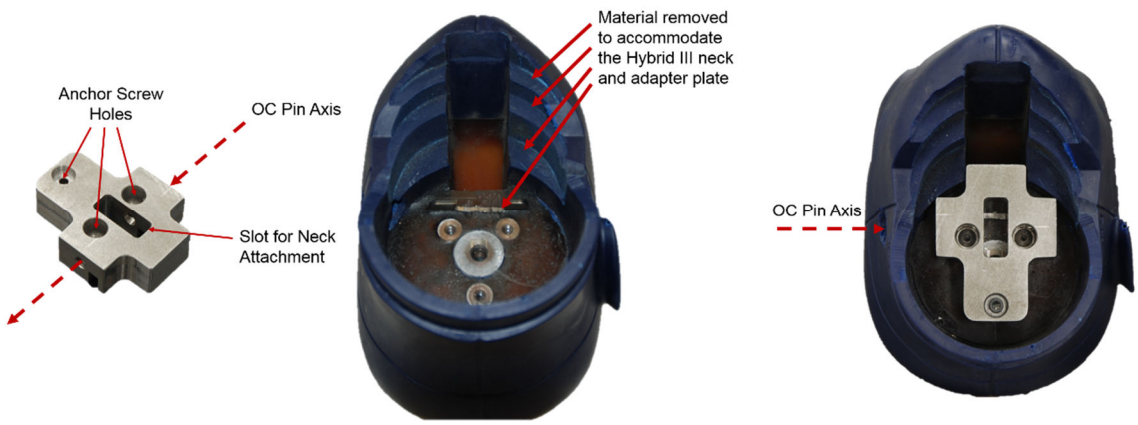

Figure 5.2: Adapter plate (left) and headform modifications (center) required to fit a NOCSAE headform to a Hybrid III neck and move the occipital condyle joint forward. Headform material was removed around the underside of the chin to accommodate the adapter plate and neck. The far right picture shows the adapter plate installed on the underside of the headform and the location where the occipital condyle (OC) pin is installed.

Kinematic data of the NOCSAE headform were collected at 20 kHz using a 6DX Pro 2k-18k six-degree of freedom (6DOF) sensor package (DTS, Seal Beach, CA). The sensor package was mounted on a custom-built aluminum block placed inside the instrumentation shaft of the NOCSAE headform placing the measurement axis 5.74 mm (0.226 in) anterior (x-axis) and 0.89 mm (0.035 in) inferior (z-axis) to the CG of the headform and rotated -20˚ about the y axis (J211 coordinate system). Accelerometer data were filtered using a CFC 1000 low-pass anti-aliasing filter in accordance with SAE J211 standard and angular rate data were filtered using a CFC 155

filter. The filter specification for angular rate data was based on a previous test series in which the peak acceleration values of the 6DOF sensor package were optimized to match those of the 3-2-2-2 arrangement. Kinematic data measured at the sensor package were rotated to match the orientation of the SAE J211 head coordinate system (Equations 5.1 and 5.2). Angular acceleration values were calculated in the rotated coordinate system (Equation 5.3) and then linear accelerations were calculated for the CG of the headform (Equation 5.4).

$$[\boldsymbol{a}]_{\boldsymbol{R}} = [\boldsymbol{a}]_M * \begin{bmatrix} \cos(\theta_y) & 0 & \sin(\theta_y) \\ 0 & 1 & 0 \\ -\sin(\theta_y) & 0 & \cos(\theta_y) \end{bmatrix} \tag{5.1}$$

$$[\boldsymbol{\omega}]_{\boldsymbol{R}} = [\boldsymbol{\omega}]_M * \begin{bmatrix} \cos(\theta_y) & 0 & \sin(\theta_y) \\ 0 & 1 & 0 \\ -\sin(\theta_y) & 0 & \cos(\theta_y) \end{bmatrix} \tag{5.2}$$

$$[\dot{\boldsymbol{\omega}}(\boldsymbol{i})] = \frac{[\boldsymbol{\omega}(\boldsymbol{i}+\mathbf{1})]_{\mathbf{0}} - [\boldsymbol{\omega}(\boldsymbol{i})]_{\mathbf{0}}}{\Delta t} \tag{5.3}$$

$$\boldsymbol{a}_{\boldsymbol{CG}} = \boldsymbol{a}_{\boldsymbol{R}} + \boldsymbol{\omega}_{\boldsymbol{R}} \times (\boldsymbol{\omega}_{\boldsymbol{R}} \times \boldsymbol{\rho}_{\boldsymbol{CG}}) + \dot{\boldsymbol{\omega}} \times \boldsymbol{\rho}_{\boldsymbol{CG}} \tag{5.4}$$

In Equations 5.1-5.4, a is acceleration (g), ω is angular rate (rad/s), $\dot{\omega}$ is angular or rotational acceleration (rad/s^2), θ_y is the angular offset (rad), i is the time step, and Δt is change in time from time step i to time step $i+1$ (0.05 ms), and ρ_{CG} is a position vector relative to the original point of measurement. The subscripts M, R, and CG designate the location and orientation of the origin: M represents the original measurement axes, R is after rotating the axes, and CG is at the center of gravity of the headform.

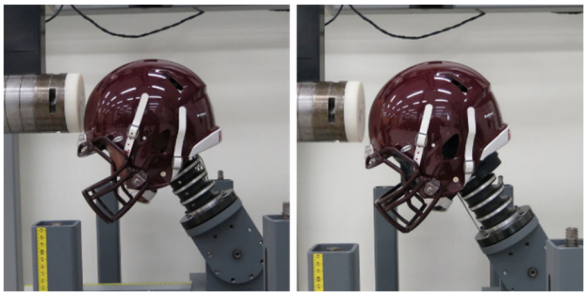

Front – Azimuth: 0˚, Elevation: 30˚

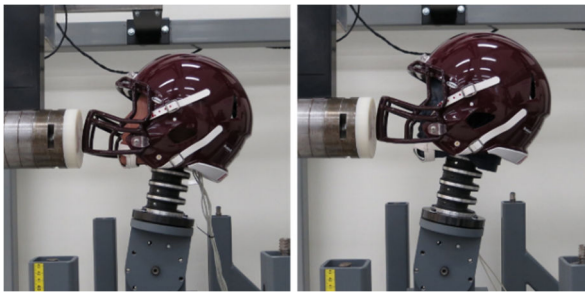

Facemask – Azimuth: 0˚, Elevation: -10˚

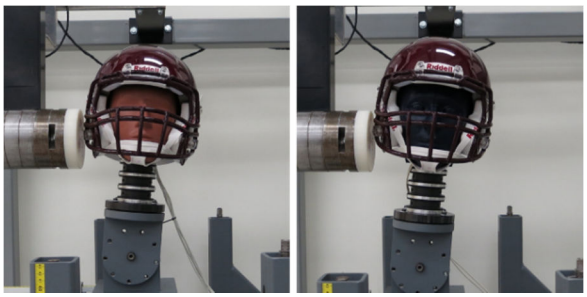

Jaw – Azimuth: -90˚, Elevation: -5˚

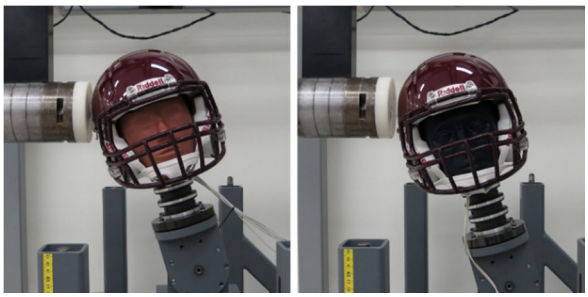

Side – Azimuth: -90˚, Elevation: 15˚

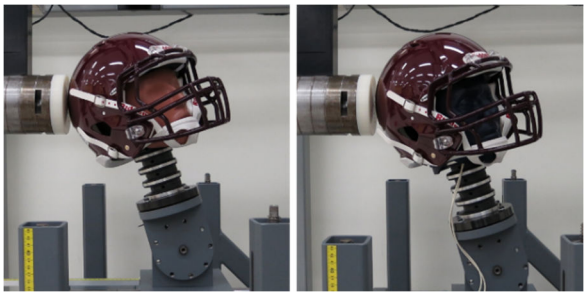

Rear-Boss – Azimuth: -135˚, Elevation: 15˚

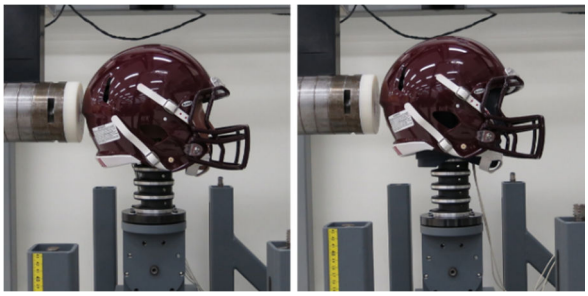

Rear – Azimuth: 180˚, Elevation: 0˚

Figure 5.3: Helmeted Hybrid III and NOCSAE headforms showing the six impact locations: front, facemask, jaw, side, rear-boss, and rear. These locations are representative of the most common head impact locations observed in on-field datasets.

Impact response was assessed using a series of parameters based on the acceleration and angular rate measurements. Linear and angular accelerations were determined for the CG of the headforms as functions of time. Peak acceleration and peak angular rate values, which are associated with the pressures and strains in the brain that have been correlated with concussion risk, were recorded.[6] The linear acceleration traces were also used to ascertain measures of impact event duration that are associated with concussion risk.[100] Time to peak linear acceleration was defined as the time from the start of the impact event to the peak linear acceleration, while event duration was the time from the start of the impact event to the time of peak resultant linear velocity. The start of the impact event was defined using a 0.5 g threshold for resultant linear acceleration. The ratio of the resultant linear acceleration to the resultant angular acceleration was used to approximate the radius of rotation of the headform as a function of time.

Two other commonly used head injury metrics, Gadd Severity Index (SI) and Head Injury Criterion (HIC) were also calculated for each impact (Equations 5.6 and 5.7). [101, 102] Both SI and HIC combine weighted accelerations with duration to calculate a single number that is associated with head injury.[8, 28, 32, 82] These metrics serve as correlates to energy transferred to the head during impact.

$$SI = \int^{T} a(t)^{2.5} dt \tag{5.6}$$

$$HIC_{15} = \left\{ (t_2 - t_1) \left[\int_{t_1}^{t_2} \frac{a(t)dt}{(t_2 - t_1)} \right]^{2.5} \right\}_{max} \tag{5.7}$$

In Equations 5.6 and 5.7, T is the full event duration defined previously while t_1 is the beginning of the HIC range and t_2 is the end. HIC was determined over a maximum time window of 15 ms.

Differences between the two headforms in biomechanical magnitudes and variances among matched test conditions were assessed for all parameters. Statistical comparisons were made using a three-way analysis of variance (ANOVA) test to compare the affects impactor velocity and impact location had on the kinematic parameters of the two headforms. Post-hoc 2-way ANOVAs and Fisher's LSD tests were conducted to compare differences in parameters between the two headforms for each velocity-location combination. Repeatability among matched tests was assessed using coefficient of variance (COV), which is the ratio of the standard deviation of matched test responses and the mean, expressed as a percentage. COV values for each parameter of the two headforms were compared across all test conditions using two-sample Student's t-test. Significance was set at $\alpha = 0.05$ for all statistical analyses.

Results

Throughout the 180 tests conducted, the headforms demonstrated similar response patterns to one another for corresponding test conditions (Figures 5.4 and 5.5). The response corridors in Figures 5.4 and 5.5 show the upper and lower bounds of all repeated tests by test condition and headform. Statistical analyses using three-way ANOVAs revealed significant differences among test conditions ($p < 0.001$) for all parameters. Post-hoc analyses revealed significant differences between headform by impact velocity-location combinations for all parameters ($p < 0.001$), including linear and angular acceleration.

Linear and angular acceleration comparisons by matched location and magnitude conditions (Table 5.1) showed significant differences between headforms for several test conditions. For linear acceleration, eight out of eighteen (8/18) test conditions had significant differences. The NOCSAE headform peak linear acceleration was as much as 10.1% lower than that of the Hybrid III headform for the medium velocity jaw impacts and as much as 19.9% higher for the medium velocity facemask impacts. The angular acceleration comparisons revealed significant differences in eleven out of eighteen (11/18) test conditions. As with linear acceleration, the largest differences between headforms occurred at the facemask location. No significant differences were found in COV values between the two headforms for linear (p = 0.335) or angular acceleration (p = 0.841). Relatively large variances were found for several test conditions, including the facemask, where the acceleration plots show wide corridors (Figures 5.4 and 5.5).

Differences between the headforms varied by impact location. At the front location, a significant difference in peak linear acceleration was found for the high velocity condition, where the NOCSAE headform was 9.0% higher than the Hybrid III. The Hybrid III and NOCSAE headforms had COV values of 1.7% and 3.4%, respectively, for this test condition. Larger significant differences were found at the facemask location, where the NOCSAE headform had 19.9% and 17.7% higher peak linear accelerations for the medium and high velocity conditions. Large differences were also found in the angular acceleration values, where the NOCSAE headform was 65.3% higher, 28.5% higher, and 22.5% lower than the Hybrid III for the low, medium, and high velocities. Impacts to the jaw resulted in significant differences in peak linear and angular acceleration for both the medium and high velocities. For linear acceleration, the NOCSAE headform had 10.1% lower and 4.0% lower values than the Hybrid III. The angular accelerations

of the NOCSAE headform were 26.9% higher and 25.3% higher than the Hybrid III for the medium and high velocity conditions. For side impacts, no significant differences were found in peak linear acceleration. The NOCSAE headform did have 9.1% higher angular acceleration for the medium velocity. At the rear-boss location, the only significant difference was for peak linear acceleration at the high velocity condition, where the NOCSAE headform acceleration was 8.0% higher than that of the Hybrid III. Several significant differences were found at the rear impact location, where differences in peak linear acceleration were found for the medium and high velocities, and differences in peak angular acceleration were found at all three velocities. The differences at the rear location ranged from 7.2% for linear acceleration at the high velocity condition to 29.4% for angular acceleration at the medium velocity.

Condition-specific significant differences were also found in all the other parameters when comparing headforms with matched magnitude and location conditions in all of the other parameters ($p < 0.001$). No significant differences were found between the headforms in COV values. COV and mean percent differences are summarized in Table 5.2 for all parameters.

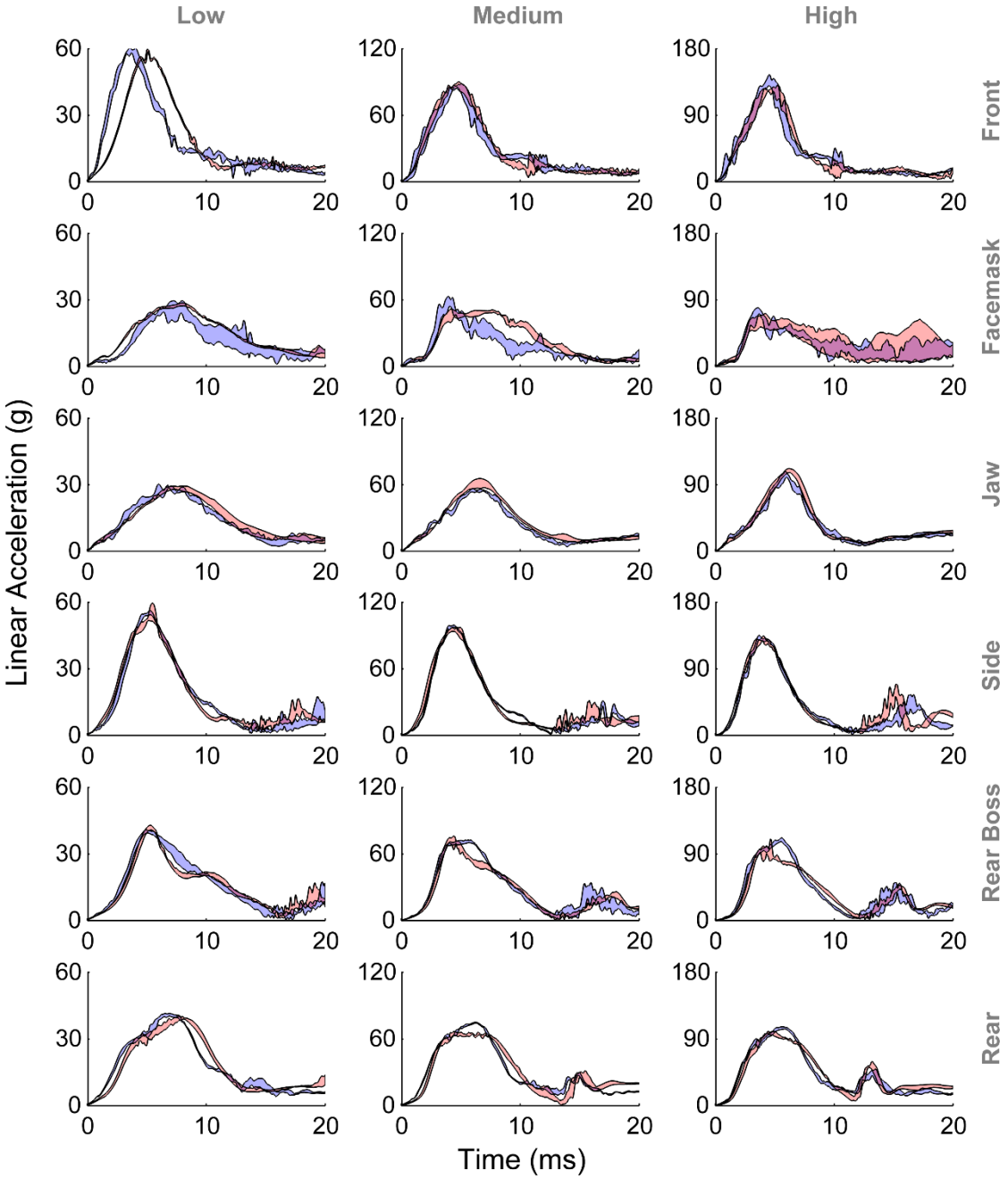

Figure 5.4: Linear acceleration time traces for each velocity (columns) and location (rows) for the Hybrid III (red) and NOCSAE (blue) headforms. Shaded regions correspond to corridors bounded by the highest and lowest headform acceleration responses at each instant in time (relative to the start of the events) for the respective headform. The acceleration traces show good agreement headforms and repeatability for all test conditions except those at the facemask location.

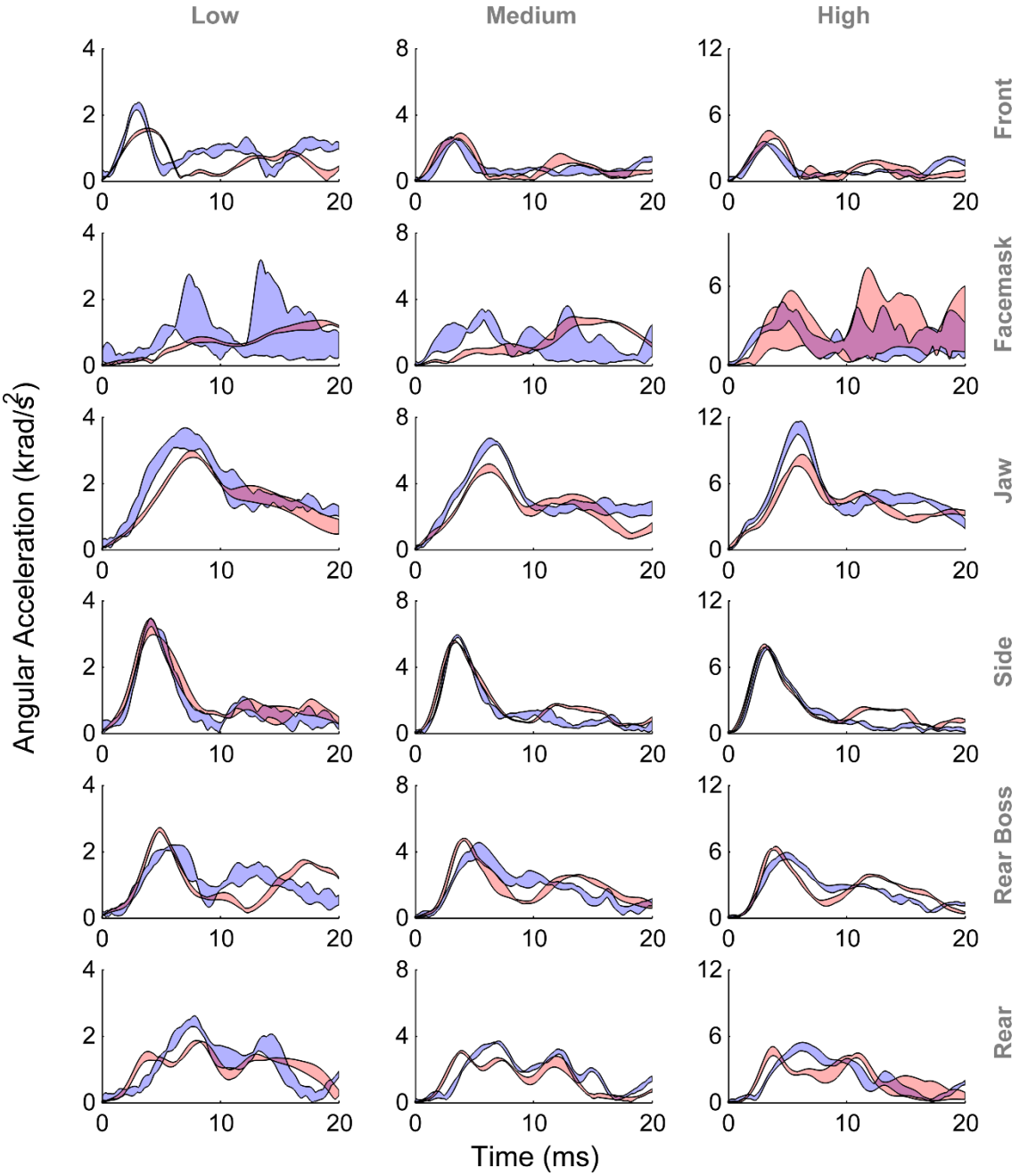

Figure 5.5: Angular acceleration time traces for each velocity (columns) and location (rows) for the Hybrid III (red) and NOCSAE (blue) headforms. Shaded regions correspond to corridors bounded by the highest and lowest headform acceleration responses at each instant in time (relative to the start of the events) for the respective headform. The acceleration traces show good agreement between repeated tests and headform for most test conditions.

Table 5.1: Summary of peak linear and angular acceleration comparisons between the Hybrid III and NOCSAE headforms for each test condition. The coefficient of variance (COV) for peak acceleration values of matched tests were similar for the two headforms. Differences between headforms were quantified as mean difference in peak acceleration (Δ). Positive values of Δ indicate larger NOCSAE headform values. Condition-specific significant differences were identified between headforms (denoted by *).

	Peak Linear Acceleration (g)					Peak Angular Acceleration (krad/s^2)				
	Hybrid III	COV (%)	NOCSAE	COV (%)	Δ	Hybrid III	COV (%)	NOCSAE	COV (%)	Δ
Front										
Low	59.5 ± 0.4	0.6	59.6 ± 0.7	1.2	0.0	1.70 ± 0.11	6.5	2.29 ± 0.08	3.4	0.59 *
Medium	88.8 ± 1.1	1.2	87.1 ± 1.5	1.7	-1.7	2.65 ± 0.12	4.5	2.55 ± 0.08	3.2	-0.10
High	128.1 ± 2.2	1.7	139.6 ± 4.7	3.4	11.5 *	4.09 ± 0.29	7.1	3.47 ± 0.09	2.5	-0.62 *
Facemask										
Low	28.1 ± 0.4	1.5	28.5 ± 1.2	4.0	0.4	1.50 ± 0.07	4.8	2.48 ± 0.66	26.6	0.98 *
Medium	50.3 ± 1.0	1.9	60.4 ± 3.2	5.3	10.0 *	2.82 ± 0.15	5.4	3.62 ± 0.28	7.8	0.80 *
High	63.2 ± 6.2	9.8	74.3 ± 3.0	4.1	11.2 *	5.62 ± 1.09	19.3	4.36 ± 0.34	7.7	-1.27 *
Jaw										
Low	29.1 ± 0.6	2.0	29.5 ± 0.5	1.7	0.4	3.09 ± 0.07	2.1	3.43 ± 0.18	5.4	0.33
Medium	62.1 ± 3.0	4.9	55.8 ± 0.5	0.9	-6.2 *	5.18 ± 0.13	2.6	6.57 ± 0.14	2.1	1.39 *
High	109.4 ± 1.8	1.6	105.1 ± 3.0	2.9	-4.3 *	8.88 ± 0.38	4.3	11.13 ± 0.46	4.2	2.25 *
Side										
Low	53.6 ± 3.0	5.6	55.5 ± 0.6	1.0	1.8	3.04 ± 0.09	3.0	3.34 ± 0.09	2.6	0.30
Medium	95.6 ± 1.4	1.4	98.1 ± 0.6	0.6	2.5	5.41 ± 0.11	2.0	5.91 ± 0.06	1.0	0.50 *
High	129.8 ± 2.4	1.9	132.1 ± 2.1	1.6	2.3	7.92 ± 0.13	1.6	7.71 ± 0.11	1.5	-0.20
Rear Boss										
Low	41.8 ± 0.7	1.6	40.4 ± 0.5	1.3	-1.4	2.43 ± 0.08	3.4	2.14 ± 0.06	2.7	-0.29
Medium	74.5 ± 1.6	2.1	71.6 ± 1.1	1.5	-3.0	4.25 ± 0.24	5.7	4.02 ± 0.30	7.5	-0.23
High	100.9 ± 5.0	5.0	109.0 ± 1.6	1.5	8.1 *	5.67 ± 0.16	2.7	5.67 ± 0.23	4.0	0.00
Rear										
Low	39.7 ± 0.4	1.0	41.1 ± 0.4	1.0	1.4	1.88 ± 0.10	5.2	2.43 ± 0.11	4.7	0.55 *
Medium	66.0 ± 0.7	1.1	74.6 ± 0.3	0.4	8.6 *	2.92 ± 0.06	1.9	3.65 ± 0.05	1.2	0.73 *
High	98.2 ± 1.3	1.3	105.2 ± 0.9	0.9	7.0 *	4.46 ± 0.26	5.8	4.99 ± 0.29	5.7	0.53 *

Table 5.2: Averaged percent difference in magnitude between headforms for various parameters, and corresponding COV values for each headform. No significant differences were identified between headforms in COV values.

	Percent difference in magnitude	COV	
		Hybrid III	NOCSAE
Peak Linear Acceleration	3.7 ± 7.8	2.6 ± 2.3	2.0 ± 1.4
Peak Angular Acceleration	12.0 ± 21.6	4.9 ± 4.0	5.2 ± 5.8
Time to Peak	-1.5 ± 18.3	6.4 ± 6.7	3.6 ± 2.2
Event Duration	14.2 ± 33.8	2.2 ± 2.7	2.0 ± 2.3
Peak Angular Rate	-7.9 ± 12.6	2.9 ± 3.5	2.1 ± 2.5
HIC	-5.6 ± 19.5	3.2 ± 3.8	4.1 ± 5.7
SI	-12.2 ± 12.8	2.7 ± 2.4	3.1 ± 4.6
Radius of Rotation	-4.1 ± 33.9	11.6 ± 11.9	9.7 ± 9.6

Discussion

This test series offers a comprehensive helmeted head impact response comparison for the Hybrid III and NOCSAE headforms. The results have application toward future helmet evaluation standards and protocols. While both headforms have been used extensively for helmet testing in the past, no direct comparisons had been conducted to define how tests results may differ from one headform to the other. This comparison will contribute to the development of improved helmet evaluation protocols to optimize helmets in order to further reduce concussion risk in helmeted sports.[103] The results show test condition-specific differences in kinematic data between the two headforms that should be considered when selecting a headform for helmet testing and evaluation. In terms of repeatability, the Hybrid III and NOCSAE headforms had similar coefficient of variation (COV) values for peak linear (μ_{HIII} = 2.6%; μ_{NOCSAE} = 2.0%) and peak angular acceleration (μ_{HIII} = 4.9%; μ_{NOCSAE} = 5.2%), which are consistent with past studies of headform response.[74, 77, 104] Both impact location and velocity affected the differences between headforms. A greater number of significant differences were identified at higher impact velocities, likely because the higher energy impacts exaggerated response differences due to inertial properties and headform-helmet interactions.

Impact location had a more complicated effect on differences in impact response between the two headforms. Impacts that were lower on the helmet (facemask, jaw, and rear) all resulted in significant differences in peak linear acceleration for the medium and high velocities. For angular, the facemask and rear impacts resulted in significant differences at all impact velocities. Shape differences between the Hybrid III and NOCSAE headforms may have contributed to differences

in these impact locations by affecting the interaction between the headforms and helmet pads. The Hybrid III has narrower cheeks than the NOCSAE headform and the back of the headform does not extend all the way to the bottom of the football helmet pads.[105] Impacts higher on the helmet (front, side, and rear-boss) tended to show better agreement between headforms, with significant differences in linear acceleration only for high velocity impacts and fewer significant differences in angular acceleration.

The facemask impacts resulted in some of the largest differences between headforms and COV values. In addition to headform shape, facemask deformation also substantially affected these results. As stated previously, the Hybrid III has narrower cheeks than the NOCSAE headform, allowing for more space between the helmet cheek pads and the face and helmet movement relative to the headform. Interestingly, impacts to the facemask resulted in lower peak linear acceleration values compared to other locations. The difference is likely due to the energy absorption and modulation associated with facemask deformation. At the highest impact magnitude, the facemask peak linear accelerations were nearly 30% lower than all other locations and resulted in permanent facemask deformation. Without the facemask impacts, the average percent difference between the headforms for linear acceleration would be 1.8 ± 6.0% and angular acceleration would be 9.6 ± 15.9%. The COV values would also decrease: linear acceleration COV values would be 2.2 ± 1.6% and 1.4 ± 0.8% for the Hybrid III and NOCSAE headforms while angular acceleration COV values would be 3.9 ± 1.8% and 3.4 ± 1.8%.

Linear acceleration results showed small differences between the headforms in terms of peak values and variation between matched tests. While significant differences were found between the two headforms for peak linear acceleration values in eight out of eighteen impact conditions, the average difference across all conditions was just 3.7%. The largest differences between the headforms occurred at the facemask location, where facemask deformation affected helmet fit and energy transfer to the headform. A second interesting finding was observed in the low magnitude impacts to the front location, where the Hybrid III time traces ramp up slowly for the first few milliseconds. The difference in response at this test condition may be due to energy absorption early in the impact by the rubber nodding blocks used for the Hybrid III headform. At the medium and high magnitudes, the effect due to nodding blocks may not be substantial enough to be observed in the plots (Figures 5.4 and 5.5). No significant differences were found between the two headforms in average coefficient of variance (COV) values of peak linear acceleration. These linear acceleration results show that helmeted impact tests conducted using a NOCSAE headform mounted on a Hybrid III neck differ from those conducted using a Hybrid III headform for some impact conditions; though, on average, the differences are small and the two test set ups are similarly repeatable. Given that only small differences were found, these results suggest that both headforms provide reasonable impact responses in terms of linear acceleration.

Differences between the two headforms for angular acceleration were larger than those observed for linear acceleration, likely due to differences in inertial properties and helmet fit. In general, the same angular acceleration patterns were observed in the time traces (Figures 5.4 and 5.5) of the two headforms, particularly during the first 10 ms of the events. As with the linear acceleration results, the largest differences were observed at the facemask location and can likely be attributed

to the same issues associated with facemask deformation noted in the discussion of linear acceleration data. Averaged across all test conditions, the NOCSAE headform had 12.0 ± 21.6% higher peak angular acceleration than the Hybrid III and significant differences were found at eleven out of eighteen conditions. Average COV values were significantly higher for angular acceleration for both headforms compared to the linear acceleration conditions (p = 0.043; p = 0.031), though no significant differences were observed between the two headforms.

For the other parameters, average differences tended to be small relative to standard deviations, and the differences were similar in magnitude to those observed for peak linear and angular accelerations. COV values were also in line with those observed for peak acceleration values for most parameters. Time to peak linear acceleration for the Hybrid III headform had a large average and standard deviation of COV values that can be attributed primarily to impacts to the facemask, where some COV values topped 20%. Radius of rotation had the highest average COV for both headforms. The high variance of the radius of rotation term is due to the contributions of variance from both peak linear and angular acceleration at the time of peak linear acceleration.

While some differences in impact response were identified between the Hybrid III and NOCSAE headforms, these differences do not indicate that one headform is superior to the other for helmeted impact testing. Rather, the results demonstrate two important findings: (1) the two headforms have similar levels of repeatability, (2) the two headforms produce similar, though not identical results. These two findings suggest that either headform is likely to consistently produce reasonable head impact response results for helmeted impacts, albeit they may not produce the same results. Given

that both headforms offer acceptable accuracy and repeatability, other factors such as shape and helmet fit should be considered when selecting a headform for testing. The NOCSAE headform more closely resembles the shape of a human head, likely leading to a more realistic head-helmet interaction compared to the Hybrid III.[41] Helmets designed to maximize scores on evaluations utilizing the Hybrid III headform may not offer proper fit or the same level of protection for athletes in the field that helmets designed for NOCSAE headform tests could offer.

This study has limitations that affect how these data can be interpreted. A limited number of impact locations, directions, and magnitudes were tested. While the test conditions were selected based on data collected in the field, they do not fully represent all the possible impact conditions that football players may experience.[11, 27] The six test locations used in this study represent common impact locations from the on-field data, while the test magnitudes span the range of higher impact magnitudes observed in on-field datasets, including concussive impacts. There were some challenges in setting the same impact locations for the two headforms. While the impactor face was aligned to a common marker on the helmets, differences in helmet fit could have affected the alignment. Furthermore, differences between the relative locations of CG and OC joint for the headforms likely had an effect on the directions of the impacts. Only one helmet type and one of each headform type was used for testing, as testing more helmets and headforms would have been impractical, though other football helmets and helmets from other sports may affect the headform responses in different ways. Each helmet model modulates the transfer of energy to the head in a slightly different way but the same patterns in head kinematics would likely be observed regardless of helmet type. This study did not investigate the effects other factors such as temperature, humidity, impactor face, or helmet age may have on headform response.[64, 106]

Conclusion

This study assessed differences in head impact response between the Hybrid III and NOCSAE headforms in helmeted pendulum impact tests. The results showed test condition-specific differences in average response for all parameters though the differences tended to be small. In terms of linear and angular acceleration, the NOCSAE headform demonstrated slightly higher values on average: 3.7 ± 7.8% for linear acceleration and 12.0 ± 21.6% higher for angular acceleration. For matched test conditions, the two headforms showed similar levels of variability for all parameters. Many of the largest differences between the two headforms were associated with impacts to the helmet facemask, where headform shape and facemask deformation likely contributed to elevated levels of variability. Without the facemask impacts, the NOCSAE headform had on average 1.8 ± 6.0% higher peak linear and 9.6 ± 15.9% higher peak angular acceleration. The two headforms demonstrated similar levels of variance for all testing conditions. While the two headforms demonstrated similar and similarly-consistent impact response results, the NOCSAE headform, which is shaped more like a human head, is a better option for testing protocols used to evaluate helmet performance.

Chapter 6: Conclusions

The studies presented in this dissertation have contributed to the body of knowledge on sports-related concussions by looking at both field and laboratory methods employed to study brain injury. While much more research is required to combat the issue, these studies provide valuable information that will be used to reduce the occurrence of concussions in sports.

No single approach will solve the concussion issue because many factors affect head impact exposure and injury risk. Rather, a broad approach that addresses rule changes, improved technique, and better equipment is necessary to minimize sports-related concussions. The first two studies (Chapters 2 and 3) investigated head impact exposure in youth football and the methods used to collect this exposure data. In Chapter 2, on-field data were used to assess the effects of rule changes on head impact exposure in youth football while in the future they will be used to evaluate helmets for young players. The last two studies (Chapters 4 and 5) focused on laboratory protocols aimed at maximizing the performance of helmets so as to provide athletes with the best protection from head injury that equipment can provide. Future research should continue to address all three aspects of injury prevention to minimize the incidence of concussions in sports.

Youth athletes make up the majority of participants in sports, including collision sports like football where concussions are most prevalent. The first study presented in this dissertation (Chapter 2) was the first to characterize head impact exposure for 9 to 12 year old football players. This study was also the first to quantify the effects rules to limit contact in practice have on head impact exposure. The results demonstrated a significant reduction in the number of head impacts players sustained during the season for teams that limited contact in practice. Future studies are needed to further characterize head impact exposure at this level; in particular, data that can relate head impact exposure to injury and functional changes in the brain in young athletes are needed.

Advances in laboratory methods to make helmet testing protocols more representative of real-world conditions are essential for continued improvement in athletic helmets. Testing methods that incorporate three-dimensional kinematics are of particular interest. The last two studies presented in this dissertation (Chapters 4 and 5) investigated two of the most commonly used headforms for helmet testing in order to guide researchers in the development of new testing procedures that include three-dimensional kinematics. These studies found that the National Operating Committee on Standards for Athletic Equipment (NOCSAE) headform is a better representation of a human head than the Hybrid III in terms of shape though both the headforms produce reasonable kinematic responses in impacts. The NOCSAE headform is a better option than the Hybrid III for helmeted head impacts in most cases because of the more realistic shape that leads to better helmet fit.

The studies presented in this dissertation have all been submitted to peer reviewed journals for publication. A summary of publications is provided in Table 6.1.

Table 6.1: Summary of dissertation publications.

Chapter	Title	Journal	Status
2	Head Impact Exposure in Youth Football: Elementary School Ages 9 to 12 Years and the Effect of Practice Structure	Annals of Biomedical Engineering	Accepted
3	Quantifying the Effects of Random Measurement Error on Descriptive Statistics of Biomechanical Datasets	Annals of Biomedical Engineering	In-review
4	Quantitative Comparison of Hybrid III and NOCSAE Headform Shape Characteristics	Journal of Sports Engineering and Technology	Accepted
5	Comparative Analysis of Helmeted Impact Response of Hybrid III and NOCSAE Headforms	Journal of Sports Engineering and Technology	In-review

References

1. Langlois JA, Rutland-Brown W and Wald MM. The epidemiology and impact of traumatic brain injury: a brief overview. *The Journal of head trauma rehabilitation*. 2006; 21: 375-8.

2. Gilchrist J, Thomas K, Xu L, McGuire L and Coronado V. Nonfatal traumatic brain injuries related to sports and recreation activities among persons aged≤ 19 years-United States, 2001-2009. *Morbidity and Mortality Weekly Report*. 2011; 60: 1337-42.

3. Stern RA, Riley DO, Daneshvar DH, Nowinski CJ, Cantu RC and McKee AC. Long-term consequences of repetitive brain trauma: chronic traumatic encephalopathy. *PM&R*. 2011; 3: S460-S7.

4. Guskiewicz KM, Marshall SW, Bailes J, et al. Recurrent concussion and risk of depression in retired professional football players. *Medicine and science in sports and exercise*. 2007; 39: 903-9.

5. McCrory P, Meeuwisse WH, Aubry M, et al. Consensus statement on concussion in sport: the 4th International Conference on Concussion in Sport held in Zurich, November 2012. *British journal of sports medicine*. 2013; 47: 250-8.

6. Hardy WN, Mason MJ, Foster CD, et al. A study of the response of the human cadaver head to impact. *Stapp car crash journal*. 2007; 51: 17-80.

7. Greenwald RM, Gwin JT, Chu JJ and Crisco JJ. Head impact severity measures for evaluating mild traumatic brain injury risk exposure. *Neurosurgery*. 2008; 62: 789-98; discussion 98.

8. Duma SM, Manoogian SJ, Bussone WR, et al. Analysis of real-time head accelerations in collegiate football players. *Clin J Sport Med*. 2005; 15: 3-8.

9. Rowson S, Brolinson G, Goforth M, Dietter D and Duma SM. Linear and angular head acceleration measurements in collegiate football. *Journal of biomechanical engineering*. 2009; 131: 061016.

10. Rowson S and Duma SM. Development of the STAR Evaluation System for Football Helmets: Integrating Player Head Impact Exposure and Risk of Concussion. *Ann Biomed Eng*. 2011; 39: 2130-40.

11. Rowson S and Duma SM. Brain Injury Prediction: Assessing the Combined Probability of Concussion Using Linear and Rotational Head Acceleration. *Ann Biomed Eng*. 2013.

12. Rowson S, Duma SM, Beckwith JG, et al. Rotational head kinematics in football impacts: an injury risk function for concussion. *Ann Biomed Eng*. 2012; 40: 1-13.

13. Guskiewicz KM and Mihalik JP. Biomechanics of sport concussion: quest for the elusive injury threshold. *Exerc Sport Sci Rev*. 2011; 39: 4-11.

14. Broglio SP, Schnebel B, Sosnoff JJ, et al. Biomechanical properties of concussions in high school football. *Medicine and science in sports and exercise*. 2010; 42: 2064-71.

15. Broglio SP, Surma T and Ashton-Miller JA. High school and collegiate football athlete concussions: a biomechanical review. *Ann Biomed Eng*. 2012; 40: 37-46.

16. Crisco JJ, Wilcox BJ, Beckwith JG, et al. Head impact exposure in collegiate football players. *Journal of biomechanics*. 2011; 44: 2673-8.

17. Crisco JJ and Greenwald RM. Let's get the head further out of the game: a proposal for reducing brain injuries in helmeted contact sports. *Current sports medicine reports*. 2011; 10: 7-9.

18. Rules Changes Regarding Practice & Concussion Prevention. Pop Warner 2012.

19. *Sports-Related Concussions in Youth: Improving the Science, Changing the Culture*. The National Academies Press, 2013.

20. Benson BW, McIntosh AS, Maddocks D, Herring SA, Raftery M and Dvořák J. What are the most effective risk-reduction strategies in sport concussion? *British journal of sports medicine*. 2013; 47: 321-6.

21. Daniel RW, Rowson S and Duma SM. Head Impact Exposure in Youth Football. *Ann Biomed Eng*. 2012; 40: 976-81.

22. Broglio SP, Sosnoff JJ, Shin S, He X, Alcaraz C and Zimmerman J. Head impacts during high school football: a biomechanical assessment. *Journal of athletic training*. 2009; 44: 342-9.

23. Crisco JJ, Fiore R, Beckwith JG, et al. Frequency and location of head impact exposures in individual collegiate football players. *Journal of athletic training*. 2010; 45: 549-59.

24. Crisco JJ, Wilcox BJ, Machan JT, et al. Magnitude of head impact exposures in individual collegiate football players. *Journal of applied biomechanics*. 2012; 28: 174-83.

25. Funk JR, Rowson S, Daniel RW and Duma SM. Validation of Concussion Risk Curves for Collegiate Football Players Derived from HITS Data. *Ann Biomed Eng*. 2012; 40: 79-89.

26. Guskiewicz KM, Mihalik JP, Shankar V, et al. Measurement of head impacts in collegiate football players: relationship between head impact biomechanics and acute clinical outcome after concussion. *Neurosurgery*. 2007; 61: 1244-53.

27. Pellman EJ, Viano DC, Tucker AM and Casson IR. Concussion in professional football: location and direction of helmet impacts-Part 2. *Neurosurgery*. 2003; 53: 1328-40; discussion 40-1.

28. Pellman EJ, Viano DC, Tucker AM, Casson IR and Waeckerle JF. Concussion in professional football: reconstruction of game impacts and injuries. *Neurosurgery*. 2003; 53: 799-814.

29. Viano DC, Withnall C and Halstead D. Impact performance of modern football helmets. *Ann Biomed Eng*. 2012; 40: 160-74.

30. Viano DC and Halstead D. Change in size and impact performance of football helmets from the 1970s to 2010. *Ann Biomed Eng*. 2012; 40: 175-84.

31. Viano DC, Withnall C and Wonnacott M. Effect of mouthguards on head responses and mandible forces in football helmet impacts. *Ann Biomed Eng*. 2012; 40: 47-69.

32. Viano DC, Withnall C and Wonnacott M. Football Helmet Drop Tests on Different Fields Using an Instrumented Hybrid III Head. *Ann Biomed Eng*. 2012; 40: 97-105.

33. Duma SM and Rowson S. Past, present, and future of head injury research. *Exerc Sport Sci Rev*. 2011; 39: 2-3.

34. Guskiewicz KM, Weaver NL, Padua DA and Garrett WE, Jr. Epidemiology of concussion in collegiate and high school football players. *The American journal of sports medicine*. 2000; 28: 643-50.

35. Powell JW and Barber-Foss KD. Traumatic brain injury in high school athletes. *Jama*. 1999; 282: 958-63.

36. Manoogian S, McNeely D, Duma S, Brolinson G and Greenwald R. Head acceleration is less than 10 percent of helmet acceleration in football impacts. *Biomedical sciences instrumentation*. 2006; 42: 383-8.

37. Crisco JJ, Chu JJ and Greenwald RM. An algorithm for estimating acceleration magnitude and impact location using multiple nonorthogonal single-axis accelerometers. *Journal of biomechanical engineering*. 2004; 126: 849-54.

38. Beckwith JG, Greenwald RM and Chu JJ. Measuring Head Kinematics in Football: Correlation Between the Head Impact Telemetry System and Hybrid III Headform. *Ann Biomed Eng*. 2012; 40: 237-48.

39. Schnebel B, Gwin JT, Anderson S and Gatlin R. In vivo study of head impacts in football: a comparison of National Collegiate Athletic Association Division I versus high school impacts. *Neurosurgery*. 2007; 60: 490-5; discussion 5-6.

40. Boden BP, Tacchetti RL, Cantu RC, Knowles SB and Mueller FO. Catastrophic head injuries in high school and college football players. *The American journal of sports medicine*. 2007; 35: 1075-81.

41. Pellman EJ, Powell JW, Viano DC, et al. Concussion in professional football: epidemiological features of game injuries and review of the literature--part 3. *Neurosurgery*. 2004; 54: 81-94; discussion -6.

42. Beckwith JG, Greenwald RM, Chu JJ, et al. Head impact exposure sustained by football players on days of diagnosed concussion. *Medicine and science in sports and exercise*. 2012.

43. Ross DT, Meaney DF, Sabol MK, Smith DH and Gennarelli TA. Distribution of forebrain diffuse axonal injury following inertial closed head injury in miniature swine. *Exp Neurol*. 1994; 126: 291-9.

44. Camarillo DB, Shull PB, Mattson J, Shultz R and Garza D. An instrumented mouthguard for measuring linear and angular head impact kinematics in American football. *Annals of biomedical engineering*. 2013; 41: 1939-49.

45. Wong RH, Wong AK and Bailes JE. Frequency, magnitude, and distribution of head impacts in Pop Warner football: The cumulative burden. *Clinical Neurology and Neurosurgery*. 2014; 118: 1-4.

46. Young TJ, Daniel RW, Rowson S and Duma SM. Head Impact Exposure in Youth Football: Elementary School Ages 7-8 Years and the Effect of Returning Players. *Clinical journal of sport medicine: official journal of the Canadian Academy of Sport Medicine*. 2014.

47. Mihalik JP, Guskiewicz KM, Marshall SW, Blackburn JT, Cantu RC and Greenwald RM. Head impact biomechanics in youth hockey: comparisons across playing position, event types, and impact locations. *Annals of biomedical engineering*. 2012; 40: 141-9.

48. Mihalik J, Guskiewicz K, Jeffries J, Greenwald R and Marshall S. Characteristics of head impacts sustained by youth ice hockey players. *Proceedings of the Institution of Mechanical Engineers, Part P: Journal of Sports Engineering and Technology*. 2008; 222: 45-52.

49. Cobb BR, Urban JE, Davenport EM, et al. Head Impact Exposure in Youth Football: Elementary School Ages 9–12 Years and the Effect of Practice Structure. *Ann Biomed Eng*. 2013; 41: 2463-73.

50. Hanlon E and Bir C. Real-time head acceleration measurement in girls youth soccer. *Medicine & Science in Sports & Exercise*. 2011.

51. Beckwith JG, Chu JJ and Greenwald RM. Validation of a noninvasive system for measuring head acceleration for use during boxing competition. *Journal of applied biomechanics*. 2007; 23: 238-44.

52. Chu JJ, Beckwith JG, Leonard DS, Paye CM and Greenwald RM. Development of a multimodal blast sensor for measurement of head impact and over-pressurization exposure. *Annals of biomedical engineering*. 2012; 40: 203-12.

53. McIntosh AS, McCrory P and Comerford J. The dynamics of concussive head impacts in rugby and Australian rules football. *Medicine and science in sports and exercise*. 2000; 32: 1980-4.

54. Cobb BR, Rowson S and Duma SM. Age-Related Differences in Head Impact Exposuire of 9-13 Year Old Football Players. *Biomedical sciences instrumentation*. 2014.

55. Landau DP and Binder K. A guide to Monte Carlo simulations in statistical physics. Cambridge University Press, 2009.

56. Newman JA, Beusenberg MC, Shewchenko N, Withnall C and Fournier E. Verification of biomechanical methods employed in a comprehensive study of mild traumatic brain injury and the effectiveness of American football helmets. *Journal of biomechanics*. 2005; 38: 1469-81.

57. Niehoff P and Gabler HC. The accuracy of WinSmash delta-V estimates: the influence of vehicle type, stiffness, and impact mode. *Annual Proceedings/Association for the Advancement of Automotive Medicine*. Association for the Advancement of Automotive Medicine, 2006, p. 73.

58. Elliott B and Alderson J. Laboratory versus field testing in cricket bowling: A review of current and past practices in modelling techniques. *Sports Biomechanics*. 2007; 7: 99-108.

59. Stöggl T, Lindinger S and Müller E. Biomechanical validation of a specific upper body training and testing drill in cross-country skiing. *Sports Biomechanics*. 2006; 5: 23-46.

60. Lienhard K, Schneider D and Maffiuletti NA. Validity of the Optogait photoelectric system for the assessment of spatiotemporal gait parameters. *Medical engineering & physics*. 2013; 35: 500-4.

61. Hartmann A, Luzi S, Murer K, de Bie RA and de Bruin ED. Concurrent validity of a trunk tri-axial accelerometer system for gait analysis in older adults. *Gait & posture*. 2009; 29: 444-8.

62. Rath AL, Manoogian SJ, Duma SM, Bolton BJ and Crandall JR. An Evaluation of a Fiber Optic Based Sensor for Measuring Chest and Abdominal Deflection. *Society of Automotive Engineers*. 2005: 2005-01-0745.

63. NOCSAE. Standard Test Method and Equipment Used in Evaluating the Performance Characteristics of Protective Headgear/Equipment. National Operating Committee on Standards for Athletic Equipment, 2011.

64. Rowson S and Duma SM. The temperature inside football helmets during head impact: a five-year study of collegiate football games. *Proceedings of the Institution of Mechanical Engineers, Part P: Journal of Sports Engineering and Technology*. 2013; 227: 12-9.

65. Post A, Hoshizaki TB, Gilchrist M and Brien S. Analysis of the influence of independent variables used for reconstruction of a traumatic brain injury incident. *Proceedings of the*

Institution of Mechanical Engineers, Part P: Journal of Sports Engineering and Technology. 2012: 1754337112436629.

66. McIntosh AS, Patton DA and Thai K. Impact assessment of jockey helmet liner materials. *Proceedings of the Institution of Mechanical Engineers, Part P: Journal of Sports Engineering and Technology*. 2012: 1754337112436628.

67. Hoshizaki TB, Walsh E, Post A, et al. The application of brain tissue deformation values in assessing the safety performance of ice hockey helmets. *Proceedings of the Institution of Mechanical Engineers, Part P: Journal of Sports Engineering and Technology*. 2012: 1754337112448765.

68. Walsh ES, Post A, Rousseau P, et al. Dynamic impact response characteristics of a helmeted Hybrid III headform using a centric and non-centric impact protocol. *Proceedings of the Institution of Mechanical Engineers, Part P: Journal of Sports Engineering and Technology*. 2012: 1754337112442299.

69. Ouckama R and Pearsall DJ. Impact performance of ice hockey helmets: head acceleration versus focal force dispersion. *Proceedings of the Institution of Mechanical Engineers, Part P: Journal of Sports Engineering and Technology*. 2012: 1754337111435625.

70. Blanco DH, Cernicchi A and Galvanetto U. Design of an innovative optimized motorcycle helmet. *Proceedings of the Institution of Mechanical Engineers, Part P: Journal of Sports Engineering and Technology*. 2014: 1754337113518748.

71. Hodgson VR. National Operating Committee on Standards for Athletic Equipment football helmet certification program. *Medicine and science in sports*. 1975; 7: 225.

72. Cormier J, Manoogian S, Bisplinghoff J, et al. Biomechanical Response of the Human Face and Corresponding Biofidelity of the FOCUS Headform. *SAE Int J Passeng Cars - Mech Syst*. 2010; 3: 842-59.

73. Foster JK, Kortge JO and Wolanin MJ. Hybrid III~ A Biomechanically-Based Crash Test Dummy. *Proceedings of the 21st Stapp Car Crash Conference*. 1977; SAE 770938.

74. Kendall M, Walsh ES and Hoshizaki TB. Comparison between Hybrid III and Hodgson–WSU headforms by linear and angular dynamic impact response. *Proceedings of the Institution of Mechanical Engineers, Part P: Journal of Sports Engineering and Technology*. 2012; 226: 260-5.

75. Bartsch A, Benzel E, Miele V and Prakash V. Impact test comparisons of 20th and 21st century American football helmets. *J Neurosurg*. 2012; 116: 222-33.

76. Rousseau P, Post A and Hoshizaki T. The effects of impact management materials in ice hockey helmets on head injury criteria. *Proceedings of the Institution of Mechanical Engineers, Part P: Journal of Sports Engineering and Technology*. 2009; 223: 159-65.

77. Walsh ES, Rousseau P and Hoshizaki TB. The influence of impact location and angle on the dynamic impact response of a hybrid III headform. *Sports Engineering*. 2011; 13: 135-43.

78. Gwin JT, Chu JJ, Diamond SG, Halstead PD, Crisco JJ and Greenwald RM. An investigation of the NOCSAE linear impactor test method based on in vivo measures of head impact acceleration in American football. *Journal of biomechanical engineering*. 2010; 132: 011006.

79. NOCSAE. Standard linear impactor test method and equipment used in evaluating the performance characteristics of protective headgear and face guards. National Operating Committee on Standards for Athletic Equipment, 2006.

80. NOCSAE. Standard Projectile Impact Test Method and Equipment Used in Evaluating the Performance Characteristics of Protective Headgear, Faceguards or Projectiles. National Operating Committee on Standards for Athletic Equipment, 2009.

81. NOCSAE. Standard Performance Specification for Newly Manufactured Football Helmets. National Operating Committee on Standards for Athletic Equipment, 2011.

82. Pellman EJ, Viano DC, Withnall C, Shewchenko N, Bir CA and Halstead PD. Concussion in professional football: helmet testing to assess impact performance--part 11. *Neurosurgery*. 2006; 58: 78-96; discussion 78-96.

83. Hanlon E and Bir C. Validation of a wireless head acceleration measurement system for use in soccer play. *Journal of applied biomechanics*. 2010; 26: 424-31.

84. McIntosh AS and McCrory P. Impact energy attenuation performance of football headgear. *British journal of sports medicine*. 2000; 34: 337-41.

85. Hubbard RP and McLeod DG. Definition and Development of A Crash Dummy Head. *Proceedings of the 18th Stapp Car Crash Conference*. 1974; SAE 741193.

86. Hubbard R and McLeod D. A basis for crash dummy skull and head geometry. *Human Impact Response-Measurement and Simulation, Plenum Press, New York, NY,[319]*. 1973.

87. Hertzberg H, Daniels GS and Churchill E. Anthropometry of flying personnel-1950. Wright-Patterson Air Force Base, Ohio: Wright Air Development Center, 1953.

88. Kroon D. Wavefront OBJ toolbox. 2011.

89. Gayzik FS, Moreno DP, Vavalle NA, Rhyne AC and Stitzel JD. Development of a Full Human Body Finite Element Model for Blunt Injury Prediction Utilizing a Multi-Modality Medical Imaging Protocol. *12th Int'l LS-DYNA User Conf*. 2012.

90. Fitting Instructions and Helmet Care. *Riddell*.

91. MacAlister A, Young TJ, Daniel RW, Rowson S and Duma S, M. Methodology for Mapping Football Head Impact Exposure to Helmet Pads for Repeated Loading Testing. *Biomedical sciences instrumentation*. 2014.

92. Viano DC and Pellman EJ. Concussion in professional football: biomechanics of the striking player--part 8. *Neurosurgery*. 2005; 56: 266-80; discussion -80.

93. Rowson S, Beckwith JG, Chu JJ, Leonard DS, Greenwald RM and Duma SM. A six degree of freedom head acceleration measurement device for use in football. *Journal of applied biomechanics*. 2011; 27: 8-14.

94. King AI, Yang KH, Zhang L, Hardy W and Viano DC. Is Head Injury Caused by Linear or Angular Acceleration? *Proceedings of the International Research Conference on the Biomechanics of Impact (IRCOBI)*. Lisbon, Portugal2003.

95. Hirsch AE and Ommaya AK. Protection from Brain Injury: The Relative Significance of Translational and Rotational Motions of the Head after Impact. *SAE Technical Paper Series*. 1970; 700899: 144-51.

96. Beyer JA, Rowson S and Duma SM. Concussions experienced by major league baseball catchers and umpires: field data and experimental baseball impacts. *Ann Biomed Eng*. 2012; 40: 150-9.

97. Padgaonkar AJ, Kreiger KW and King AI. Measurement of Angular Acceleration of a Rigid Body Using Linear Accelerometers. *J Appl Mech*. 1975; 42: 552-6.

98. Cobb BR, MacAlister A, Young TJ, Kemper AR, Rowson S and Duma SM. Quantitative Comparison of Hybrid III and NOCSAE Headform Shape Characteristics and Implications on Football Helmet Fit. *Proceedings of the Institution of Mechanical Engineers, Part P: Journal of Sports Engineering and Technology*. 2014; DOI: 10.1177/1754337114548245.

99. Young TJ, Daniel RW, Rowson S and Duma SM. Head Impact Exposure in Youth Football: Elementary School Ages 7-8 Years and the Effect of Returning Players. *Clinical Journal of Sport Medicine*. 2013.

100. Ommaya AK. Biomechanics of Head Injuries: Experimental Aspects. In: Melvin ANaJW, (ed.). *Biomechanics of Trauma*. Eat Norwalk, CT: Appleton-Century-Crofts, 1985.

101. Gadd CW. Use of a weighted-impulse criterion for estimating injury hazard. *Proceedings of the 10th Stapp Car Crash Conference*. 1966; SAE 660793.

102. Versace J. A Review of the Severity Index. *SAE Technical Paper Series*. 1971; SAE 710881.

103. Rowson S, Duma SM, Greenwald RM, et al. Can helmet design reduce the risk of concussion in football? Technical note. *Journal of neurosurgery*. 2014; 120: 919-22.

104. Siegmund GP, Guskiewicz KM, Marshall SW, DeMarco AL and Bonin SJ. A headform for testing helmet and mouthguard sensors that measure head impact severity in football players. *Annals of biomedical engineering*. 2014; 42: 1834-45.

105. Cobb BR, MacAlister A, Young TJ, Kemper AR, Rowson S and Duma SM. Quantitative comparison of Hybrid III and National Operating Committee on Standards for Athletic Equipment headform shape characteristics and implications on football helmet fit. *Proceedings of the Institution of Mechanical Engineers, Part P: Journal of Sports Engineering and Technology*. 2014: 1754337114548245.

106. Rowson S, Daniel RW and Duma SM. Biomechanical performance of leather and modern football helmets: Technical note. *Journal of neurosurgery*. 2013; 119: 805-9.